CARBON FIBER-CEMENT ADHESION IN CARBON FIBER REINFORCED CEMENT (CFRC)

By

BRENT KEVIN LARSON

A THESIS

Submitted to
Michigan State University
in partial fulfillment of the requirements
for the degree of

MASTER OF SCIENCE

Department of Chemical Engineering

1988

ABSTRACT

CARBON FIBER-CEMENT ADHESION IN CARBON FIBER REINFORCED CEMENT (CFRC)

By

BRENT KEVIN LARSON

The addition of short carbon fibers to cement causes a great increase in the composite material tensile, flexural, and impact strength, and toughness. The purpose of this research is to understand how cement properties are improved by carbon fibers and to understand what level of adhesion and interfacial failure mode are necessary to obtain optimum carbon fiber reinforced cement (CFRC) properties.

Various admixtures were included in CFRC and their effects on the carbon fiber-cement adhesion and the composite material properties were determined using a pull-out test and a flexural test.

Latex and hot water curing dramatically increase the fiber-matrix adhesion. Both latex with anti-foam agent and hot water curing increase flexural strength by 40% over normal CFRC, and latex increases toughness 100%. Manipulation of the fiber-matrix adhesion changes the failure mode from fiber pull-out to fiber rupture. Optimum strength and toughness result from an intermediate level of fiber-matrix adhesion.

TO LOIS ANN FOUTS,
THE ONE I WILL GO THROUGH TIME WITH,

AND TO MY PARENTS,
FOR THEIR GREAT LOVE AND ENDLESS ENCOURAGEMENT.

ACKNOWLEDGMENT

I must acknowledge the influence of the Lord Jesus Christ on my life. He is a constant source of strength and encouragement.

This research was accomplished at the Composite Materials and Structures Center at Michigan State University. I want to thank Dr. L. T. Drzal and Dr. P. Sorousian for their support, assistance, and patience during my work. I am also indebted to the following individuals: Dr. Z. Bayasi, Mr. M.J. Rich, Mr. J. Kalantar, and Mr. S. Rabonbakhsh.

I wish to gratefully acknowledge the State of Michigan Excellence Funds for financially supporting this research. Additional support was provided by Ashland Petroleum Company, Dow Corning, Elkem Chemicals, Polysar, Unimin Corporation, and W.R. Grace and Company.

TABLE OF CONTENTS

LIST OF TABLES ..... *viii*

LIST OF FIGURES ..... *ix*

INTRODUCTION 1

BACKGROUND 2

CEMENTITIOUS MATERIALS 2

HYDRATION 2

MORPHOLOGY 3

POROSITY 5

TRANSITION ZONE 7

FAILURE MODE 7

FIBER REINFORCED CEMENT 8

IMPORTANCE OF ADHESION 8

ASBESTOS 9

STEEL 9

GLASS 10

SYNTHETIC 10

CELLULOSE 11

CARBON 11

FAILURE MECHANISMS 12

REVIEW OF CFRC RESEARCH 14

AGGREGATE SIZE 14

CARBON FIBER TYPE 14

VOLUME FRACTION 14
FIBER LENGTH 15
LATEX 15
SILICA FUME 15
BONDING MECHANISMS 16
1. MECHANICAL INTERLOCKING 16
2. ADSORPTION INTERACTIONS 16
EXPERIMENTAL PROCEDURE 18
EXPERIMENTAL DESIGN PART I - INTERFACE 18
EXPERIMENTAL DESIGN PART II - MATRIX 19
MATERIALS 21
CEMENT 21
SILICA SAND 21
SUPERPLASTICIZER 22
SILICA FUME 22
CARBON FIBERS 23
LATEX 24
ANTI-FOAM AGENT 24
SET RETARDER 24
PROCEDURES 25
CEMENT MIXING PROCEDURES 25
FLEXURAL SPECIMEN TESTING 25
PULL-OUT SPECIMEN TEST THEORY 25
PULL-OUT SPECIMEN PREPARATION 28
PULL-OUT SPECIMEN TESTING 30
OPTICAL ANALYSIS 30
SCANNING ELECTRON MICROSCOPE ANALYSIS 32
ELECTRON SPECTROSCOPY FOR CHEMICAL ANALYSIS

(ESCA) 32
RESULTS AND DISCUSSION 34
PART I - INTERFACE 34
WATER-BINDER RATIO 36
SUPERPLASTICIZER 40
SILICA FUME 40
LATEX 41
PART II - MATRIX 44
FIBER 44
SILICA SAND 48
HOT WATER CURING 48
LATEX AND ANTI-FOAM AGENT 52
SET RETARDER 54
GENERAL RESULTS 54
SUMMARY AND CONCLUSIONS 57
PART I - INTERFACE 57
PART II - MATRIX 57
GENERAL 58
APPENDIX A CFRC MIXING PROCEDURE 59
APPENDIX B CALCULATIONS 60
MIX DESIGN 60
MODULUS OF RUPTURE 60
FLEXURAL STIFFNESS 61
REFERENCES 62

LIST OF TABLES

Table 1	Experimental Design	20
Table 2	Composition of Type I Portland Cement	21
Table 3	200 Mesh Silica Sand Size Distribution by Weight	22
Table 4	Composition of Grade EMS 960 Silica Fume	23
Table 5	Results of Pull-out Test and Flexural Test for Mixes 1 to 4	37
Table 6	Results of Pull-out Test and Flexural Test for Mixes 5 to 10	45

LIST OF FIGURES

Figure 1	Schematic Model of C-S-H in Cement Paste: (a) Well-Crystallized Clay Mineral; (b) Poorly Crystallized C-S-H [5]	4
Figure 2	Relationship Between Compressive Strength and Water/Cement Ratio [8]	6
Figure 3	Failure Mechanism in Fiber Reinforced Brittle Materials [34]	13
Figure 4	Critical Length Method of Determining Interfacial Bond Strength [60]	27
Figure 5	Fiber Holder Mold	29
Figure 6	To Scale Schematic Diagram of a Pull-Out Specimen	31
Figure 7	Tensile Test Jig	31
Figure 8	Length Distribution of "1.6 mm" Long Carboflex Fibers	35
Figure 9	Diameter Distribution of "1.6 mm" Long Carboflex Fibers	35
Figure 10	Pull-out and Flexural Specimen Results	38
Figure 11	Carboflex Carbon Fiber "As Received"	39
Figure 12	Carbon Fiber Pulled Out of Mix 1	39
Figure 13	Carbon Fiber Pulled Out of Mix 2	42
Figure 14	Carbon Fiber Pulled Out of Mix 3	42
Figure 15	Carbon Fiber Pulled Out of Mix 4	43
Figure 16	Close-Up of Latex-Modified Cement Adhered to Fiber	43
Figure 17	Pull-out and Flexural Specimen Results	46
Figure 18	Normalized Load Vs. Displacement	47
Figure 19	Carbon Fiber Pulled Out of Mix 7	49
Figure 20	Flexural Specimen Fracture Surface of Mix 7	49
Figure 21	Flexural Specimen Fracture Surface of Mix 8	51
Figure 22	Flexural Specimen Fracture Surface of Mix 8	51
Figure 23	Flexural Specimen Fracture Surface of Mix 9	53
Figure 24	Flexural Specimen Fracture Surface of Mix 9	53
Figure 25	Bond Strength Vs. Flex. Stiffness	55

INTRODUCTION

The addition of small amounts of short carbon fibers to cement causes a great increase in toughness, tensile strength, flexural strength, and impact strength. Carbon fiber reinforced cement (CFRC) resists crack growth under tensile stress. The carbon fibers inhibit crack propagation yielding dramatically improved cementitious composite material properties. The purpose of this research is to understand why cement properties are improved by carbon fibers and to understand which interface conditions are necessary to obtain optimum CFRC properties.

This research problem was studied in four stages. First, the geometric properties of the carbon fibers were determined and the fiber surface chemistry was obtained by x-ray photoelectron spectroscopy. Then a fiber pull-out test was developed for measuring the carbon fiber-cement interfacial shear bond strength. Third, the effects of various constituents and curing on the bond strength and composite material properties were determined using this fiber pull-out test and a bulk flexural test. Finally, the failure modes and interfacial phenomenon were studied through scanning electron microscopic examination of fracture surfaces.

BACKGROUND

To understand a composite material the constituent materials must be understood. The fiber, matrix, and interphase make important contributions to composite material properties which must be considered in predicting these properties. Thus, it is appropriate to begin with a discussion of the matrix material.

CEMENTITIOUS MATERIALS

Cementitious composites are receiving intense interest as structural materials because of their combination of physical properties, low cost and high durability. World use of hydraulic cements exceeds one billion tons annually, and it has been proposed that use could double in the next fourteen years. [1] Hydraulic cements include cement paste (cement), produced by adding water to portland cement, mortar when small aggregates (usually sand) are included, and concrete when large aggregates are added.

HYDRATION Regardless of the presence of aggregates, hydrated cement paste (HCP) refers to the phase resulting from the addition of water to portland cement. Much of the strength of HCP is derived from the hydration of calcium silicates. Di- and tri-calcium silicate ($2C_2S$ and $2C_3S$) combine with water (H) to produce calcium silicate hydrate ($C_3S_2H_3$) and calcium hydroxide (CH), as shown in the following equations written using shorthand notation.

$2C_3S + 6H \text{ ---> } C_3S_2H_3 + 3CH$

$2C_2S + 4H \text{ ---> } C_3S_2H_3 + CH$

where

$C = CaO$

$S = SiO_2$

$H = H_2O$

The composition of the hydrate is variable; $C_3S_2H_3$ is only an average molecular formula, thus the material is referred to as C-S-H. It is poorly crystalline, forming particles smaller than 1 micron. [2]

The hydration reactions of portland cement predominantly occur over a period of 24 hours. The reactions continue for years, but after 24 hours they are diffusion controlled, hence very slow. The rate of reaction is also sensitive to temperature. [3] As the temperature increases, the rate of reaction increases. Unfortunately, the structure of the HCP formed at higher temperature is not as good as that formed at lower temperatures. Hence, the short term strength of high temperature cured concrete is superior to room temperature cured concrete, but after 1 year the room temperature cured concrete is superior. [4]

MORPHOLOGY CSH is a very nearly amorphous material of indefinite morphology. Current theory holds that C-S-H has a degenerate clay structure, with calcium silicate sheets irregularly oriented, as shown in Figure 1 b). C-S-H has very poorly crystalline structure compared with clay, which has well oriented sheets of silicate and alumina held together with metal ions, as shown in Figure 1 a). [5]

The variation in spacing between the sheets yields different types of pores which affect the movement of water through the pore structure. Water in capillary pores (P) is called bulk water and is easily removed. At relative humidities below 50%, water is removed from micropores (M). Interlayer pores (I) occur where the

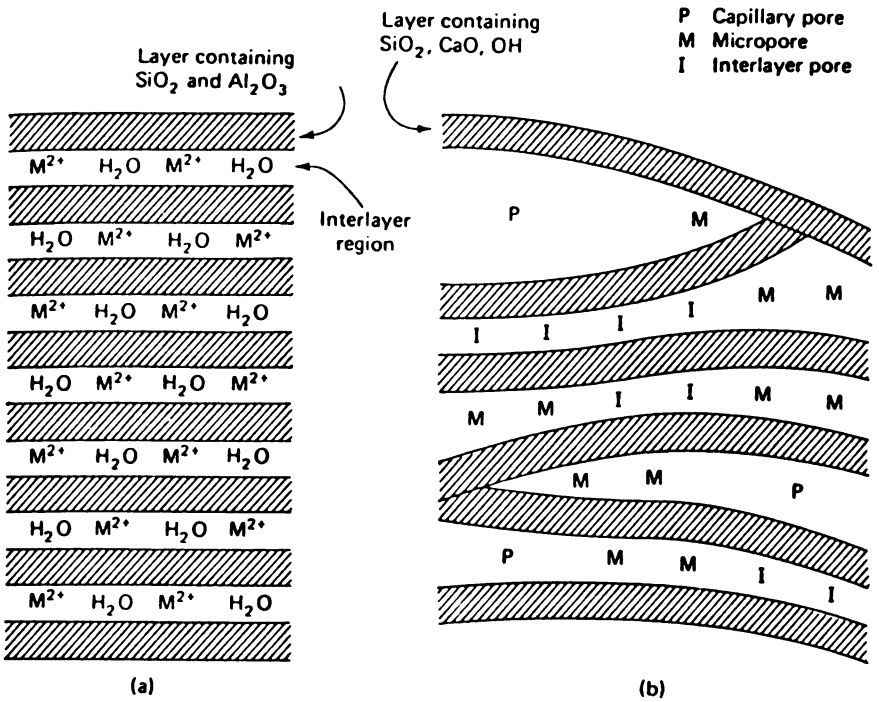

Figure 1 Schematic Model of C-S-H in Cement Paste: (a) Well-Crystallized Clay Mineral; (b) Poorly Crystallized C-S-H [5]

sheets are very close together. The water in these pores is difficult to remove. [6]

As water is removed from cement, shrinkage occurs because water no longer holds the calcium silicate layers apart. This shrinkage results in microcracking at stress concentrations throughout the matrix. Thus, before any load is applied to the cement, very small cracks are present. These cracks will propagate when the cement is placed under a mechanical load.

POROSITY Porosity is the most important factor governing the strength of brittle materials. The chemistry of the cement is not as important as the porosity. A simple two phase model explains the importance of porosity, where HCP and air are the phases. The air adds no strength to the cement, hence the higher the air content, the lower the composite material strength. This model gives the proper trend, but neglects the fact that air voids play an important role in the failure mode of cement, which will be discussed later. [7]

The porosity of hydrated cement paste is determined by the water/cement ratio for properly compacted concrete and a known degree of hydration. Figure 2 illustrates a principle known as "Abrams' water/cement ratio law". It shows the relationship between compressive strength and the water/cement ratio for constant mix proportions and maturity. A water/cement ratio of approximately 17% is required to provide enough water for chemical reaction. Some additional water is required in order to obtain reasonable workability, but this water merely adds to the porosity of the mix, lowering the concrete strength. Thus, the overall trend illustrated by Figure 2 shows an inverse relationship between compressive strength and water/cement ratio. At very low water/cement ratios, compaction becomes difficult due to low workability, and compressive strength decreases rapidly for incompletely compacted concrete as the water/cement ratio decreases. Air voids are included in the matrix in incompletely compacted concrete. Again the impact of air voids on the failure mode is seen, which will be discussed later. [8]

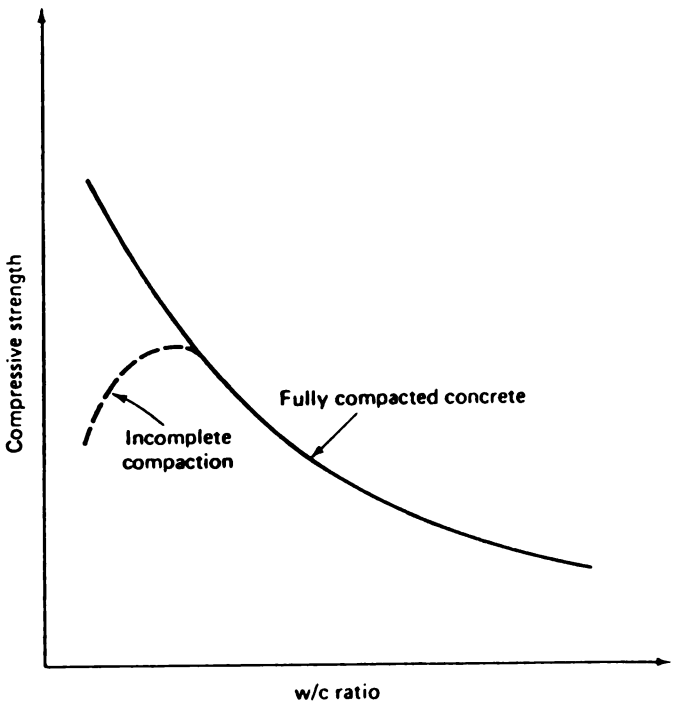

Figure 2 Relationship Between Compressive Strength and Water/Cement Ratio [8]

TRANSITION ZONE Another structural feature of concrete is the transition zone. The transition zone is an interphase, a region of changing chemical and physical properties, between the aggregate and bulk cement paste. This interphase is formed when a water film is created around aggregates. The locally higher water/cement ratio causes the crystals of hydrated cement paste to be larger than they are in the bulk. Because larger crystals don't pack as well as small crystals, the porosity in the transition zone is higher, therefore the interphase strength is lower. The transition zone composed of larger crystals and voids is the weak link between the cement matrix and the aggregate. [9]

FAILURE MODE The failure of brittle materials such as cement, mortar, and concrete is governed by a process of microcracking in which the transition zone plays an important part. As previously mentioned, when cementitious materials set and dry, shrinkage cracking occurs. Microcracks are present throughout the material even though no external load has been applied to the specimen. Cracking in cementitious materials is the result of local tensile stress. Thus, application of compressive load to a specimen results in cracking from tensile stresses due to poisson's expansion perpendicular to the loading direction. Likewise, concrete flexural specimens fail in the region of tensile stress. [10]

The failure mode involves three phases: crack initiation, slow crack growth, and rapid crack growth. Cracks may be initiated at an interphase or any flaw in the matrix. Most of the shrinkage microcracks occur in the transition zone, because this zone is weaker than the bulk paste, which is weaker than the typical aggregate. Growth of microcracks is not detectable in compressive loading until the stress is greater than 30% of the ultimate strength. At this point, the cracks begin to slowly propagate, but they primarily remain in the transition zone. Slight nonlinearity may be detected in the compression stress-strain curve in the range from 30 to 50% of the ultimate strength. Between 50 and 75% of the ultimate strength the cracks slowly

propagage into the matrix, and cracks begin to connect from one transition zone to the next. At this stress level, cracks initiated at flaws in the matrix begin to slowly propagate. Non-linearity in the stress-strain curve becomes more pronounced. Beyond 75% of the ultimate strength, crack growth is rapid. As cracks begin to connect, the rate of crack propagation increases dramatically, and failure is catastrophic. [11]

FIBER REINFORCED CEMENT

Because cementitious materials are brittle, they have been reinforced with a variety of materials in an attempt to reduce catastropic failure and increase toughness. Biblical citations from Moses' time record that bricks were made with straw. More recently, horse hair has been used to reinforce plaster. Nearly a century ago, asbestos fibers were added to portland cement to produce a revolutionary new material, asbestos fiber reinforced cement (FRC). Various methods for including wire segments or metal chips in concrete are nearly as old. [12] Technology has recently allowed production of a wide variety of synthetic fibers which have been considered as reinforcements for portland cement. [13] At present, the types of reinforcing fibers used with cements include asbestos, steel, glass, nylon, polypropylene, polyethylene, aramid, polyester, acrylic, cellulose, and carbon. The benefits of reinforcement include improvements in: crack resistance, strength, toughness, impact energy absorption, wear durability, ductility, and dimensional stability. Other constituents may be added to produce lightweight materials.

IMPORTANCE OF ADHESION Good fiber-matrix adhesion is required for each of these reinforcements in FRC to improve cement properties. A strong bond allows load transfer from the matrix to the fibers. This load transfer is important when the specimen is drying as well as when it is loaded. If the fiber-matrix bond is poor, added reinforcements are merely inclusions in the matrix, sites for matrix

failure.

Study of the fiber-matrix bond is complicated by the fact that the cement matrix is inhomogeneous. The chemistry, morphology, and physical properties of the matrix change as a function of distance from the reinforcement with many types of fiber. This layer of material with changing properties as a function of distance is called an interphase.

ASBESTOS Asbestos cement was widely used, but its use is rare now because of a perceived health risk. Asbestos FRC has much improved flexural strength and toughness compared with non-fibrous cement. The superior properties are the result of very good fiber-cement adhesion. Mechanical interlocking between asbestos fibers and hydrated cement has been shown to be an important interfacial bonding mechanism in asbestos-cement composites. [14] Addition of silica fume has been shown to improve fiber-matrix bond strength. [15]

STEEL Steel fibers have been used to reinforce cement for the past 20 years. They approximately double the cost of cement, but their use is increasing because of the great increase in toughness, impact resistance, erosion resistance, and strength provided by these fibers. The most efficient method of improving interfacial bonding between steel fibers and matrix is to mechanically deform the end of the fiber to achieve positive anchorage in the matrix. Alternatively, the bonding with straight fibers may be improved by decreasing the amount of mixing water used. Addition of silica fume, expected to increase the bond strength due to increased fiber-matrix contact, has no effect on the interfacial bond strength [16], but improves the flexural strength and toughness of steel FRC. [17] Addition of more sand to the cement mix increases the fiber-matrix bond strength. [18] Longer curing times in a humid environment increases the bond strength because the interphase matrix continues to hydrate. [19] Besides fiber-matrix bonding, the frictional resistance developed with fiber pull-out is an important toughening mechanism in steel FRC. [20]

An interphase also exists in steel FRC. Bentur et al. report that the steel fiber-cement interphase consists of three layers: 1} a "duplex" film (1 to 2 microns thick) of calcium hydroxide with a single layer of calcium silicate hydrate (CSH), 2} a layer of large calcium hydroxide crystals 10 to 30 microns thick, and 3} an adjacent very porous weak interphase layer, which increases in density with distance away from the fiber. The thickness of this layer is not known. [21]

GLASS Alkali-resistant glass fibers are attractive reinforcements for cement since they are inexpensive, but the composite made from them loses strength and toughness with time. This strength loss may be due to mechanisms other than chemical attack by alkalies according to Kawamura et al. [22] They observed that the surface of the glass fibers are not etched in cement, but damage from chemical attack (though not observable with a scanning electron microscope) could occur at small surface flaws and explain the composite strength loss. Another theory is that CSH is deposited in the free spaces between fibers, causing tension in the fibers. This stress causes a loss of strain capability in the fibers, which could result in a loss of composite material strength. [23] Majumdar reports that the interfacial bond is partly chemical, with OH- ions attacking the Si-O bond in glass, weakening the fiber surface and creating strength reducing flaws. [24]

SYNTHETIC Synthetic fibers have been produced with a wide range of properties. Because of low cost, FRC with synthetic fibers has recently gained major attention. Polypropylene, nylon, and polyethylene fibers have been shown to withstand the harsh alkali environment of cement, while polyester, acrylic, and aramid fibers loose strength in the cement matrix. Polyester FRC strength loss is dramatic. Acrylic FRC is only slightly affected at room temperature, but at 50°C the loss is significant. [25] Aramid FRC cured in room temperature water shows a 15% strength decrease comparing the two year strength with the 28 day strength. [26] Because of inertness to the cement environment, polypropylene, nylon, and

polyethylene show the most promise as reinforcements for FRC.

CELLULOSE Natural fibers such as cellulose (wood) are receiving special attention because they are a renewable resource in addition to being inexpensive. The water content of the wood fibers changes the properties of the wood FRC from having greater strength (dry fibers fracture), to having greater toughness (wet fibers pull out). Hydrogen bonds and/or hydroxide bridges have been shown to play a major role in cellulose fiber-cement bonding. [27]

CARBON Carbon fibers are a superior choice as reinforcement in FRC for many applications because of their high strength, chemical inertness, size, excellent thermal stability (necessary for autoclaving), and good adhesion to cementitious matrices.

Carbon fiber reinforced cement (CFRC) was first researched by M.A. Ali and A.J. Majumdar in the 1970's. Their research was conducted with continuous polyacrylonitrile-based carbon fibers. In 1980 the Kajima Corporation added chopped, pitch-based carbon fibers to cement. Compared with ordinary cement, they found that this new composite material had high tensile strength, flexural strength, toughness, and durability, with low shrinkage. [28]

Carbon fibers improve cementitious composites in many ways. Drying of cementitious composites results in shrinkage-induced microcracking. In CFRC, the formation of shrinkage microcracks is reduced, yielding a material with few matrix defects, creating a CFRC matrix vastly improved over a non-fibrous cement matrix. [29] CFRC has a flexural strength 5 to 7 times that of the unreinforced matrix [30], which makes it a good material for use in thin sheets, such as curtain walls on buildings or floor panels. [31] CFRC is also finding application in repair work where high impact strength is important. For lightweight applications, low density aggregate may be added in addition to carbon fiber to produce a material with a specific gravity of 1.2 to 1.3 and a flexural strength of 7.5 to 11 MPa. [32]

FAILURE MECHANISMS When cementitious materials are loaded in flexure, failure is the result of the propagation of cracks initiating from microcracks or other flaws in the matrix. The matrix cracks when the tensile load at some stress concentration exceeds the tensile strength of the matrix. In fiber reinforced matrices, a crack propagates until it crosses a fiber. If the driving force behind the crack is small, the fiber may absorb enough energy to halt the crack propagation. The fiber may cause the crack to diverge into multiple cracks with less energy. These failure mechanisms result in good strength and high energy absorption (toughness) during the fracture process. [33]

If the crack has sufficient energy, it will go around the fiber and continue to propagate. For simplicity, consider a two-dimensional view of the crack, as in Figure 3. Consider the fibers with the greatest ability to inhibit crack propagation, those perpendicular to the crack propagation direction. In this case the fibers bridge the crack. Debonding begins on both sides of the crack as a result of Poisson's contraction in the fiber. The fiber transfers the tensile load across the crack, so the tensile stress in the fiber is greater than that of the matrix surrounding the fiber near the crack.

The fiber embedded length (Le) is the distance from the crack surface to the end of the fiber. Two embedded lengths which divide the local failure mechanism into three modes have been given names. If Le is less than the pull-out length (Lp), then debonding is complete and instantaneous, resulting in the fiber pulling out of the matrix. If Le is greater than Lp but less than the critical length (Lc), debonding extends gradually, eventually reaching the end of the fiber, when fiber pull-out commences. If Le is greater than Lc, debonding begins, but eventually the fiber fractures. [34]

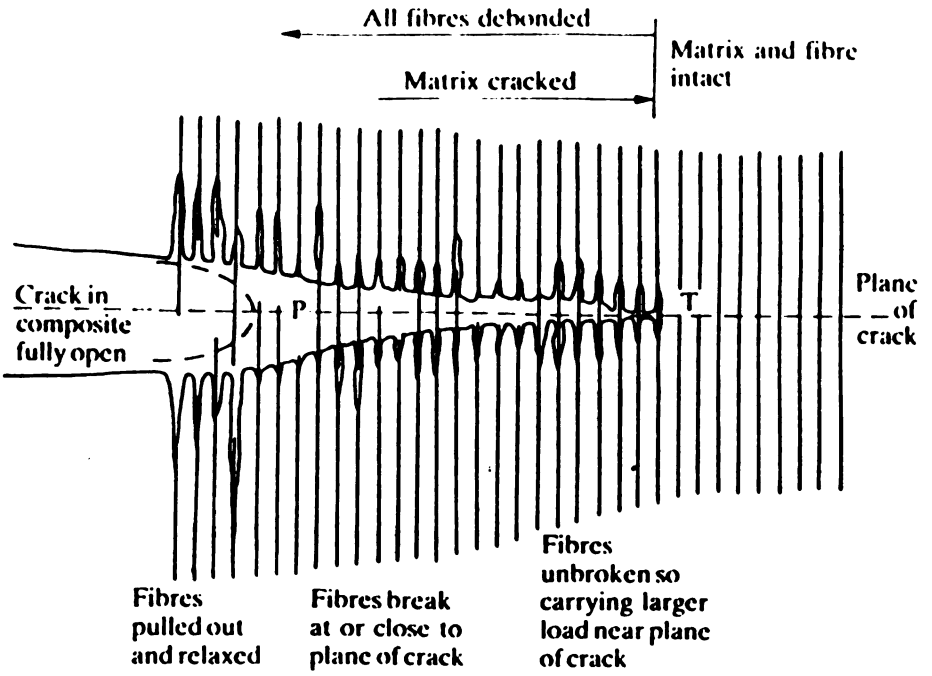

Figure 3 Failure Mechanism in Fiber Reinforced Brittle Materials [34]

REVIEW OF CFRC RESEARCH

CFRC is a complex mixture of components resulting in an exceptional material. The effects of such variables as aggregate size, carbon fiber type, volume fraction of fiber, fiber length, latex, superplasticizer, and silica fume have been studied by previous investigators.

AGGREGATE SIZE Experiments to determine the effect of aggregate size on cement show that the optimum aggregate size is less than 0.15 mm. [35] This size does not interfere significantly with the fiber dispersion, yielding a uniform, well reinforced matrix.

CARBON FIBER TYPE Carbon fiber properties influence the CFRC behavior. Polyacrylonitrile-based carbon fibers and pitch-based carbon fibers are the two types most commonly used in FRC. The polyacrylonitrile-based fiber is stronger than the pitch-based fiber by a factor of four, but the polyacrylonitrile-based carbon FRC was only 1.3 to 2.0 times as strong in tension as the pitch-based carbon FRC. [36] Because polyacrylonitrile-based fiber costs approximately four times as much as the pitch-based fiber, the pitch-based fibers are more suitable for low cost CFRC applications. [37] [38]

VOLUME FRACTION The effect of the volume fraction of fiber to binder (Vf) on material properties was studied by Akihama, et al. Many properties of CFRC increase linearly with respect to Vf to a Vf of about 4%. Among them are: flexural strength, tensile strength, and toughness. Some properties decrease linearly with Vf such as: flow (workability), density, compressive strength, and elastic modulus. At Vf greater than 4%, material properties decrease because the normal mixing process is not capable of obtaining good fiber dispersion with such high fiber content. [39] Using an Omni-mixer Vf as high as 7% has been obtained with good fiber dispersion. [40]

FIBER LENGTH The carbon fiber length is very important to the properties of CFRC. Akihama et al. have determined that only 25 to 60% of the fiber is effectively utilized in a continuous-CFRC composite material. [41] Chopped fibers are far more efficient, and the optimum length for CFRC with a Vf of 3% is 1.6 mm (0.06 in.) for optimum flexural strength. [42] However, not all fibers are the same length, and the distribution of fiber lengths may be an important factor in the effectiveness of the fibers.

LATEX The addition of a polymer emulsion, latex, to cement improves cement strength, toughness, adhesion, waterproofness, durability, and density by producing a polymer film inside the cement pore structure. The mechanism for film formation begins with the uniform dispersion of the emulsion in the cement mixing process. As latex modified cement dries, water is removed from the latex emulsion, causing flocculation of polymer particles. The latex forms a continuous layer on the particles which make up cement. As the drying continues, the particles coalesce to produce a film over all the particles in the cement mix. This film inhibits the propogation of microcracks and improves adhesion between aggregates and cement. [43] Good aggregate-cement bonding has been shown to improve the tensile strength and toughness of concrete. [44]

Latex has been shown to be an important admixture for lightweight CFRC. Using a 5% latex to binder ratio, a Vf of 1.5%, and lightweight aggregate, a material with flexural strength of 11 MPa and specific gravity of 1.3 is obtained. Without the latex, the density of the material is 10% less, but the strength of the material is greatly reduced. [45]

SILICA FUME The replacement of some cement by silica fume has been shown to increase CFRC strength by reacting with brittle calcium hydroxide to produce C-S-H, which has much improved properties. It has been proposed that silica fume (also called microsilica) improves composite material properties by

improving the fiber-matrix bond strength. [46] The optimum silica fume to cementitious material weight ratio is reported to be 23%. Superplasticizer, a polymer which reduces the amount of water required in a cement mix, is necessary when using silica fume because the extremely small particles damage workability. The optimum superplasticizer to cementitious material weight ratio is 3.2% (using the solids content of the superplasticizer). [47]

BONDING MECHANISMS

There are two bonding mechanisms which occur at the interface between carbon fiber and cement: mechanical interlocking and adsorption interactions. These mechanisms of bonding involve both chemical and physical interactions.

1. *Mechanical Interlocking* The surface roughness of the fibers is of critical importance to mechanical interlocking between carbon fibers and cementitious matrices. Surface irregularities may act as mechanical anchors yielding high bond strengths.

2. *Adsorption Interactions* Adsorption interactions result when the materials at an interface are attracted to each other due to a chemical or physical feature of a surface. Primary interactions are ionic or covalent bonds, the transfer or sharing of electrons by atoms. The bond energies are in the range from 39 to 111 kcal/mol. Secondary interactions involve dispersion interaction between molecules and have much lower energies (2-6 kcal/mol), but operate over greater distances than primary interactions. Secondary interactions include non-polar dispersion forces (Van der Waals forces), polar-dipole interactions, and polar Lewis acid-base interactions (hydrogen bonding). Intimate contact between the two phases is required for adsorption interactions to be significant. Secondary interactions are expected to be very important in the adhesion of cement to carbon fibers.

The main bonding mechanisms which are expected in carbon fiber-cement adhesion are mechanical interlocking and adsorption interactions.

EXPERIMENTAL PROCEDURE

Previous research on CFRC has provided some important qualititive observations on the role of the carbon fiber-cement interface on CFRC properties. However, because of the physical and chemical complexity of cement, attempts were made in this study to keep as many experimental variables constant as possible. The experimental plan was divided into two parts. The first portion was constructed to assess the role of the interphase on adhesion and the second to assess the role of the matrix on adhesion. For this purpose, 200 mesh silica sand was used as the aggregate, and seven days after mixing, the composite material was tested. The workability of the mixes was kept near a flow test result of 80% by varying the amount of water added to the mixes. Thus, all of the mixes could be reasonably expected to represent "real" mixes, as opposed to working with mixes which have little processability or structural potential. The CFRC mixes used in this study always contain three volume percent carbon fibers with an average length of 1.7 mm (1/16 in), silica fume, and superplasticizer.

EXPERIMENTAL DESIGN PART I - INTERFACE

The effects of admixtures on both the matrix flexural properties and the fiber-cement interfacial shear bond strength were determined in the first portion of the research. Water, superplasticizer, silica fume, and latex effects on the bond strength

were determined using a fiber pull-out test. The effects of these admixtures on cement strength, toughness, and stiffness in flexure were determined using a third-point loading test.

The cement mix designs and curing schedules were varied in accordance with Table 1. See Appendix B for the equations used to calculate the mass of the constituents from the mass ratios of Table 1. The curing schedules were varied to yield optimum composite material properties for each mix. Mix 1, the base mix, was designed to be a simple model cement, having only the necessary components. The effect of water on bond strength is shown by a second trial of mix 1 with more water. Mix 2 was identical to mix 1 except for the addition of superplasticizer. Silica fume was added to mix 2 to yield mix 3, because silica fume will not disperse without superplasticizer. Finally, latex was added to the base mix (mix 1) to give mix 4.

EXPERIMENTAL DESIGN PART II - MATRIX

The effects of five different variables on the interfacial bond strength and matrix properties were determined in the second series of experiments. The effects of fibers, silica sand, hot water curing, anti-foam agent with latex, and set retarder were studied.

A different base (mix 5), choosen to more readily accept the addition of fibers, contained silica fume and superplasticizer to aid in fiber dispersion. Fibers were added to the base mix to create mix 6. A CFRC "standard" mix, mix 7, was made by adding silica sand to mix 6. The "standard" was hot water cured to yield mix 8. Latex and anti-foam agent were added to the "standard" in mix 9. Mix 10 contained set retarder added to mix 9.

Table 1 Experimental Design (in Percents of Mass Ratios of Constituents)

Mix#	SS/B	W/B	SP/B	SF/B	Vf	L/B	AFA/B	SR/B	Cure
1(BASE1)	75	AN							a
2	75	AN	2.0						a
3	75	AN	2.0	7.5					a
4	75	AN				5			b
5(BASE2)		AN	3.2	23					a
6		AN	3.2	23	3				a
7(STD)	75	AN	3.2	23	3				a
8	75	AN	3.2	23	3				c
9	75	AN	3.2	23	3	10	1.5		b
10	75	AN	3.2	23	3	10	1.5	0.5	b

Key (mass unless otherwise stated)
B = cementitious material (binder) = cement + silica fume
SS= 200 mesh silica sand
W = water
SP= superplasticizer
SF= silica fume
Vf= volume fraction, fiber/bulk mix
L = styrene-butadiene latex
AFA=anti-foam agent
SR= set retarder
AN= as necessary to obtain uniform workability

CURE
Cure all the specimens in air covered with plastic for 24 hours. Air at 68 ± 2F (20 ± 1C) and 24 ± 2 %RH, 100%RH chamber is at the same temperature.

a. Cure in 100%RH for 5 days

b. Cure in 100%RH for 24 hours, then 4 days in air covered with plastic

c. Cure in water at 176 ± 2F (80 ± 1C) for 24 hours, then 4 days at 100%RH

All specimens are in air covered with plastic for the final 24 hours before testing. Thus, all the specimens are cured for a total of 7 days, then tested.

MATERIALS

The choice of components and admixtures in designing cementitious materials plays a critical role in obtaining the desired material properties. The names and chemistry of each of the components used in this research are described in this section.

CEMENT Portland cement is a complex mixture of many compounds, as shown in Table 2. Cement is often referred to as "binder," because it holds together the aggregate which is always mixed with it in practical applications. Ordinary Portland cement from St. Marys Peerless Cement was used to keep the mixes as simple as possible. This cement meets the requirements of ASTM specification C-150 for type I cement.

Table 2 Composition of Type I Portland Cement

Chemical	CaO	SiO_2	Al_2O_3	Fe_2O_3	MgO	SO_3	K_2O
%	63.2	21.1	5.8	2.9	2.1	2.5	0.8

SILICA SAND The aggregate for use in CFRC must be small enough to not seriously disrupt the fiber dispersion. 200 mesh silica sand from the Unimin Corporation was used. The particle size distribution is expecially important in

cement mixes with high aggregate content. Spherical particles with a distribution of diameters pack far better than uniform diameter particles. Characterization of the distribution was accomplished by sieving the sand in a series of screens and weighing the material which did not pass through each screen. This test was performed on the 200 mesh silica sand and the results are displayed in Table 3. [48] Most of the particles have diameters less than 0.074 mm (0.0029 in).

Table 3 Unimin Corporation 200 Mesh Silica Sand Size Distribution by Weight

Screen	140	200	270	325
Weight %	2	13	55	30

SUPERPLASTICIZER Daracem-100 from W.R. Grace and Company is a superplasticizer with naphthalene formaldahyde sulfonate as the active ingredient. This is an anionic material which negatively charges the cement particles, improving particle dispersion, thus allowing the use of less mixing water. [49]

SILICA FUME Grade EMS 960 silica fume from Elkem Chemicals provides excellent fiber dispersion. Silica fume is a by-product in the production of silicon metal. The reduction of quartz with coal in electric arc furnaces leaves silica fume in the escaping gases. The chemical composition of this grade of silica fume is

described in Table 4. The surface area of silica fume is high, 20 m^2/g, due to the average particle diameter of 0.15 microns. [50]

The extreme fineness and high glass content of silica fume make it a very efficient pozzolanic material (a material reactive with cement). It reacts very efficiently with calcium hydroxide to produce calcium silicate hydrate (C-S-H). Calcium hydroxide is a brittle, crystalline material with undesirable properties, but C-S-H is nearly amorphous, and provides much of the strength of cement. [51] Silica fume increases the drying shrinkage of non-fibrous cementitious materials, but carbon fibers greatly decrease shrinkage. The opposing trends cause silica fume-modified CFRC to have low shrinkage. [52]

Table 4 Composition of Elkem Chemicals Grade EMS 960 Silica Fume

Chemical	SiO_2	C	Fe_2O_3	MgO	Al_2O_3	K_2O	Na_2O
%	96.5	1.4	0.15	0.20	0.15	0.04	0.20

CARBON FIBERS Carboflex carbon fibers were supplied by the Carbon Fiber Division of Ashland Petroleum Company. The pitch-based fibers used have a reported average length of 1.6 mm (0.063 in) and a diameter of 10 - 12 microns. These fibers have a tensile strength of 560 MPa (81 ksi), when tested with a gage length of 18 mm (0.7 in), a Young's modulus of 41 - 55 GPa (6 - 8 million psi), and

specific gravity of 1.57. [53]

LATEX Polysar Latex 1186 is an aqueous emulsion of styrene-butadiene copolymers. Latex improves cement strength, toughness, adhesion, waterproofness, durability, and density by producing a polymer film inside the cement pore structure. [54]

ANTI-FOAM AGENT Anti-Foam B Emulsion Class 2 from Dow Corning (polydimethyl siloxane) was used in this study. This material is a surface active agent which reduces the surface tension of the mix, so that bubbles generated in the mixing process burst, reducing the fraction of air voids in cement. This polymer is very non-reactive and non-polar. [55]

SET RETARDER The set retarder (Daratard 17, from W.R. Grace and Company) is a combination of glucose, ligno sulfonate, and tri-ethanol amine. These materials combine to coat cement particles and provide a physical barrier to water. The hydration reaction is therefore limited by the diffusion rate of water through the coating. This coating also gives the particles a slight negative charge, yielding superplasticizer effects. The set retarder is displaced from the surface of the cement particles (mechanism unknown) after twenty-four hours. At times greater than two days, the strength of the retarded mix is greater than the same mix without set retarder, because a better hydrated cement paste structure results from a slower rate of hydration. [56]

PROCEDURES

CEMENT MIXING PROCEDURES The cement was mixed in the three-speed Hobart mixer. The volume of each mix was 3 liters. Uniform workability was desired, so enough water was added to each mix to yield a flow table test result of approximately 80%, in accordance with ASTM 230, "Flow Table for use in Tests of Hydraulic Cement." This test measures the amount of flow of a mix when it is dropped 1.27 cm (0.5 in) ten times. Appendix A provides additional details on the procedure used for mixing cement. Six 38x38x165 mm^3 (1.5x1.5x6.5 in^3) prisms were made from each mix.

FLEXURAL SPECIMEN TESTING The flexural specimens were tested on an Material Test System (MTS) Model 880. The tests were run in accordance with ASTM standard C78, "Flexural Strength of Concrete (Using Simple Beam with Third-Point Loading)." The displacement rate used was 0.015 cm/min (0.0060 in/min).

PULL-OUT SPECIMEN TEST THEORY Four techniques are presently used to measure the strength of fiber-matrix interfacial shear bond. The fragmentation test, microdebond test, microcompression test, and fiber pull-out test provide a measure of fiber-matrix interfacial bond strength. The fragmentation test requires that the matrix be transparent, and that the ultimate strain of the matrix be significantly greater than that of the fiber. Cement does not meet these requirements. The microdebond test requires that very small beads of matrix (with diameter less than the critical length for the system) be placed on the fiber. Obtaining cement of uniform composition in such small dimensions is not possible. The microcompression test involves applying compressive load on a fiber embedded in matrix. The benefit of this test is that it may be carried out on the composite material, not a model. This test suffers from

theoretical problems because in the composite material the fibers are in tension and in this test they are in compression. The best test for measuring the interfacial shear bond strength in the carbon fiber-cement system is the pull-out test. This test is relatively simple, involving pulling fibers out of the matrix. [57] The test specimen for the pull-out test is a good model of the carbon fiber-cement system. The failure mode of CFRC involves the pulling out of fibers, and the pull-out test involves the same process, thus the pull-out test is superior to the other methods of measuring the carbon fiber-cement interfacial shear bond strength.

Two types of pull-out tests were considered for determing the fiber-matrix interfacial shear strength. The direct pull-out test is not practical for this application because fiber critical lengths are less than 0.6 mm. Use of the direct method would require producing a layer of cement less than 0.6 mm thick which would be representative of bulk cement. [58] Because of the nature of cement and the size of aggregates, thin specimens can not be made.

The indirect pull-out test, also referred to as the critical length (L_c) method, depends upon consistent fiber tensile breaking strength. This method is the best for determining high bond strengths between very small fibers and cementitious matrices. Fibers with varying lengths are embedded in a sample of the chosen matrix, as shown in Figure 4 a). When the fibers are pulled, the shorter fibers pull out, and the longer fibers rupture, as shown in Figure 4 b). Thus, the critical length (the length at which fibers begin to rupture) is determined. A force balance on the longest pulled out length of fiber yields the following equation for the average fiber-matrix interfacial shear strength:

$$\tau = d_f \sigma_f / (4 L_c)$$

d_f = fiber diameter

σ_f = fiber ultimate strength

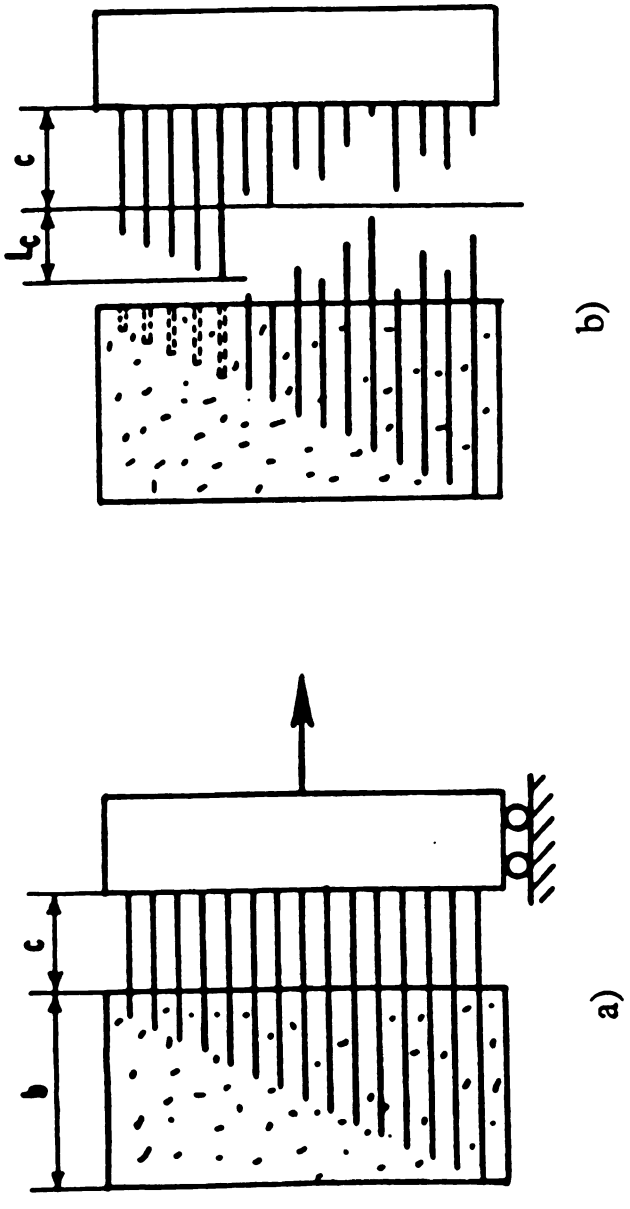

Figure 4 Critical Length Method of Determining Interfacial Bond Strength [60]

(See Appendix B for the derivation of this equation.) Only the maximum value of the average bond strength is determined using this technique. [59] This value is an average bond strength, because the bond strength varies along the length of the fiber due to the inhomogeneity of cement. Debonding causes the area of contact to be less than that assumed in this equation. Yet, because the material system is relatively constant, this test can provide a quantitiative difference in interfacial properties.

PULL-OUT SPECIMEN PREPARATION Great care was required to obtain specimens with uni-directional, equally-spaced fibers. The preparation of pull-out specimens consisted of four steps. The first three steps involve the production of fiber holders, and the last step results in the production of the pull-out specimen.

First, individual Carboflex carbon fibers were aligned in the fiber holder mold shown in Figure 5. Double-sided tape was placed on both ends of the mold to secure the fibers. Individual fibers were oriented in the mold. Ten fibers were placed in each specimen cavity in the mold. The fibers were handled at the ends, but not in the middle, so that the section of fiber which will eventually be pulled out of cement remained in the "as received" state. After all the fibers were aligned and secured, pieces of silicon mold were placed over the fibers at the ends of the mold to protect them. The fibers extending over the end of the mold were cut off.

Next, polyester was prepared and poured into the cavity in the mold. The liquid polymer sets in 30 minutes at room temperature and is completely reacted in approximately a day. Completion of the first two steps yielded rectangular pieces of polyester with fibers extending from both ends.

Third, the extending fibers were cut to the proper length. Carbon fibers have low shear strength, and are vulnerable in the fiber cutting procedure. A surgical knife was used to cut the fibers at an angle so that fiber lengths varied from as short as possible, 0.6 mm, to 1.6 mm on each specimen. A small piece of polyester was

Figure 5 Fiber Holder Mold

placed under the extending fibers to support them while they were being cut. A piece of fine grid graph paper was secured to the supporting piece of polyester to aid in obtaining the proper fiber lengths.

Finally, the fiber holders were placed in one end of a pull-out mold, with the fibers pointing toward the middle of the mold. The pull-out mold differs from a fiber holder mold only in that the piece of mold dividing the two rectangular cavities in the fiber holder mold is absent in the pull-out mold. A piece of silicone rubber was placed at the opposite end of the mold from the fiber holder to contain the cement. The cavity in the middle of the mold was filled with cement, and the cement was compacted by dropping the mold from a height of one inch ten times. Thus, cement completely filled the cavity and flowed around the fibers, yielding pull-out specimens shown schematically in Figure 6. The pull-out specimens were cured in the same manner as the flexural specimens.

PULL-OUT SPECIMEN TESTING The pull-out specimens were tested using the hand operated test jig shown in Figure 7. The specimens were secured at each end with a flat piece of metal, each of which was held in place by four screws. The screws were slowly and evenly tightened until the specimen was firmly held at both ends. A manually applied strain rate of 0.08 ± 0.03 cm/min (0.03 ± 0.01 in/min) was used for all tests. The strain resulted in a crack at the cement-polyester interface. The fibers with longer embeddment lengths fractured, and the fibers with shorter embedment lengths pulled out of the cement.

OPTICAL ANALYSIS The length and diameter distribution of the fibers used in these experiments were determined using a Joyce-Loebl Magiscan 2 optical analyzer. A small sample of fibers was dispersed in a beaker with 10 ml of ethanol and transferred to microscopic slides where they were separated from each other.

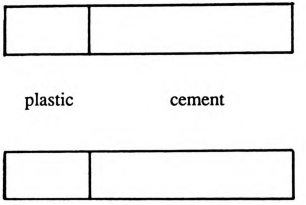

Figure 6 Schematic Diagram of a Pull-Out Specimen

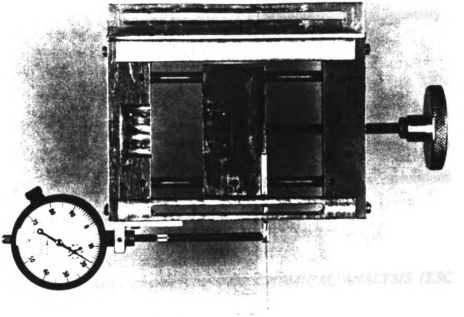

Figure 7 Tensile Test Jig

The optical analyzer captures an image from the microscope at high magnification and digitizes it. Because of the curvature of many of the fibers, the length was calculated as half of the perimeter of the fiber image. (The fiber image was reduced in width twice to eliminate the error from the diameter being included in the perimeter.)

SCANNING ELECTRON MICROSCOPE (SEM) ANALYSIS SEM is a tool which allows observation of surfaces magnifications of more than 50,000 times. An electron beam which has been accelerated through a voltage between 1 and 50 kV is focused on a surface which is to be observed using SEM. Some of the incident electrons are backscattered by the surface. Observation of the surface using these electrons is called backscattered electron imaging (BEI). Alternatively, some of the incident electrons are absorbed by surface atoms, which emit an electron. Secondary electron imaging (SEI) is accomplished using these electrons. BEI analyzes higher energy electrons than SEI. The emitted electrons are drawn to a collector which results in an emission current. This current may be amplified to intensity modulate a scanned cathode ray tube (CRT). [60]

Both flexural and pull-out specimens were observed using the SEM. Because the water present in cement outgases and interferes with the operation of the SEM, the flexural specimens were dried in a vacuum oven at a temperature of 100°C for 1 hour prior to SEM observation. Both the pull-out and flexural specimens were gold coated with a 200 angstrom layer of gold.

ELECTRON SPECTROSCOPY FOR CHEMICAL ANALYSIS (ESCA) ESCA, otherwise known as x-ray photoelectron spectroscopy (XPS), is a technique for determining surface chemistry. X-ray photons bombard a surface and cause the emission of electrons. If the photons are nearly monoenergetic, then the energy of

the electrons given off yield information about the atoms and the electronic state from which they were emitted. The energy of the incident photon is a known quantity (IPE), and the binding energy (BE) of the emitted electron can be determined because energy is conserved. The kinetic energy (KE) of the emitted energy is measured with an electron spectrometer. A correction factor or work function (WF) must be added because some of the IPE is lost to the specimen. Thus, BE = IPE - KE + WF. A plot of the number of electrons detected as a function of BE will show peaks at certain BE. The height of the peaks varies because the probability that an electron will be ejected from different orbitals varies. Each atom ejects electrons at numerous BE because the electrons come from different orbitals. [61]

The Carboflex fibers were analyzed in the "as received" state with a Perkin Elmer PHI 5400 ESCA System. The detector angle was set at 90 degrees. Elements were detected by scanning energies from 0 to 1000 eV using magnesium K_{α} radiation. The surface atomic concentrations were determined from narrow scans of the binding energies near the main element peak. The atomic concentrations were determined from ratios of the areas under the peaks.

RESULTS AND DISCUSSION

The research was divided into two portions. The first portion is focussed on the interfacial effects of admixtures, while the second portion is focussed on the effect of the interface on CFRC properties.

The carbon fiber-cement interface was characterized for mechanical strength and fracture mode using the fiber pull-out test and SEM analysis of both pull-out and flexural specimens. The cement bulk properties were obtained from third-point loading tests (flexural tests). The average carbon fiber-cement interfacial shear bond strengths, the modulus of rupture (flexural strength), flexural stiffness, and toughness (the area under the normalized load-displacement curve) were determined. These values were calculated from the equations included in Appendix B. When the results are described as being significantly different, Student's t-test shows that the results are different with a probability of 95%.

PART I - INTERFACE

First, the carbon fiber length and diameter distributions were determined. Carboflex carbon fibers with a quoted average length of 1.6 mm were analyzed with a Joyce-Loebl Magiscan 2 optical analyzer as described in the experimental procedure. The measured number average length of the carbon fibers is 1.7 mm (0.067 in), with a carbon fiber diameter of 18 ± 4 microns ($7.1 \pm 1.6 \times 10^{-4}$ in). The

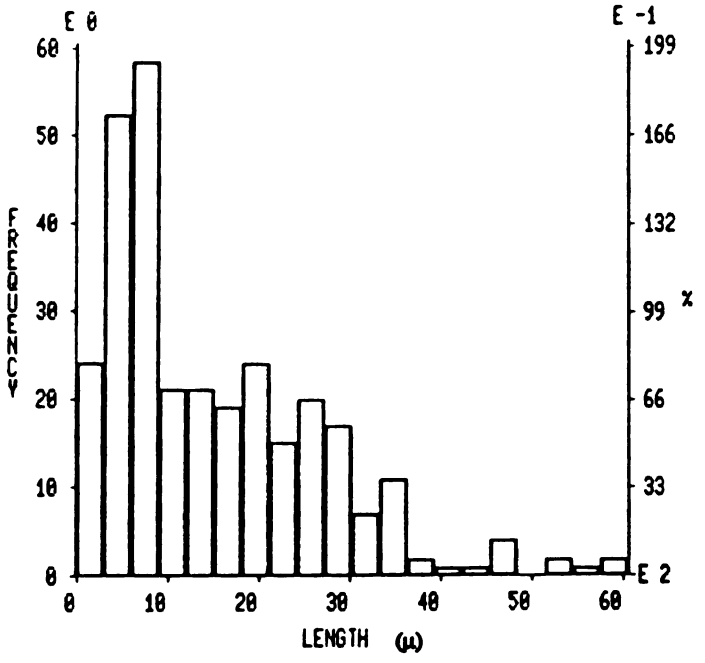

Figure 8 Length Distribution of "1.6 mm" Long Carboflex Fibers

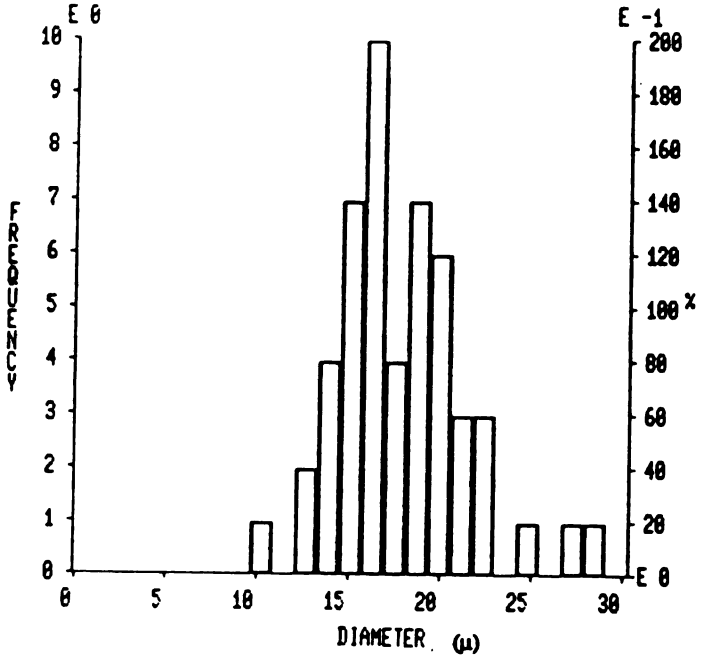

Figure 9 Diameter Distribution of "1.6 mm" Long Carboflex Fibers

length and diameter distributions of the fibers are plotted in Figures 8 and 9.

The surface chemistry of the Carboflex fibers was examined using ESCA as described in the experimental procedure. Three samples were analyzed in the "as received" state. The ESCA showed that the surface is composed of 94 ± 1 % carbon, and 5 ± 1 % oxygen. Small amounts of sodium and nitrogen were detected in one of the samples. The carbon fiber surface to which the cement adheres may be different than the surface which was analyzed, because surfaces adsorb molecules from the environment. These adsorbed molecules could be removed by the alkaline cement environment, resulting in a different carbon fiber surface for adhesion.

The effects of admixtures on both the cement matrix and the fiber-cement interface were also determined in this portion of the research. Table 5 lists the results of the interfacial and flexural tests, and Figure 10 shows this data graphically. The flexural properties of the cement are very similar, but the graph shows that the addition of latex causes a dramatic increase in carbon fiber-cement adhesion.

WATER-BINDER RATIO The effect of the water binder ratio is evident from the trials of mix 1. Higher amounts of water in this simple mix increase bond strength by decreasing the viscosity of the mix, hence improving fiber-matrix contact. Using a minimum amount of water yields optimum cement strength, but because carbon fibers are hydrophobic, the contact between the fibers and the matrix is poor. The increased mix flow increases fiber-matrix contact, yielding improved bond strength.

SEM pictures of carbon fibers pulled out of mix 1 show that very little cement remains adhered to the fibers after pull-out. Figure 11 shows a Carboflex fiber in the "as received" state, and Figure 12 shows a fiber pulled out of mix 1. Comparison of these photographs reveals that only a small amount of the surface area of the fiber is covered by cement, therefore failure occurs at the interface.

Table 5 Results of Pull-Out and Flexural Tests for Mixes 1 to 4

Mix#	Bond Strength	Toughness	Flexural Strength	Flexural Stiffness	W/B	Flow
	MPa (psi) %CV	Kg×mm (lb×in) %CV	MPa (psi) %CV	MPa/mm (ksi/in) %CV	%	%
1	2.1 (310) 26	8.2 (.71) 44	5.2 (750) 16	NA	45.5	~0
1	3.0 (440) 23	7.3 (.63) 37	3.6 (520) 12	31 (115) 26	49.7	76
1	NR	6.1 (.53) 11	3.0 (440) 11	30 (110) 14	49.7	73
2	2.7 (390) 5	11.2 (.97) 38	2.9 (430) 5	20 (75) 27	31.0	87
3	2.1 (300) 30	3.8 (.33) 24	1.3 (190) 16	7 (27) 30	32.5	102
4	>5.9 (850)	7.3 (.63) 14	2.8 (410) 24	21 (76) 3	43.5	64

Key
W/B = Water to Binder Mass Ratio
Flow = Result of Flow Test
%CV = Percent Coefficient of Variation

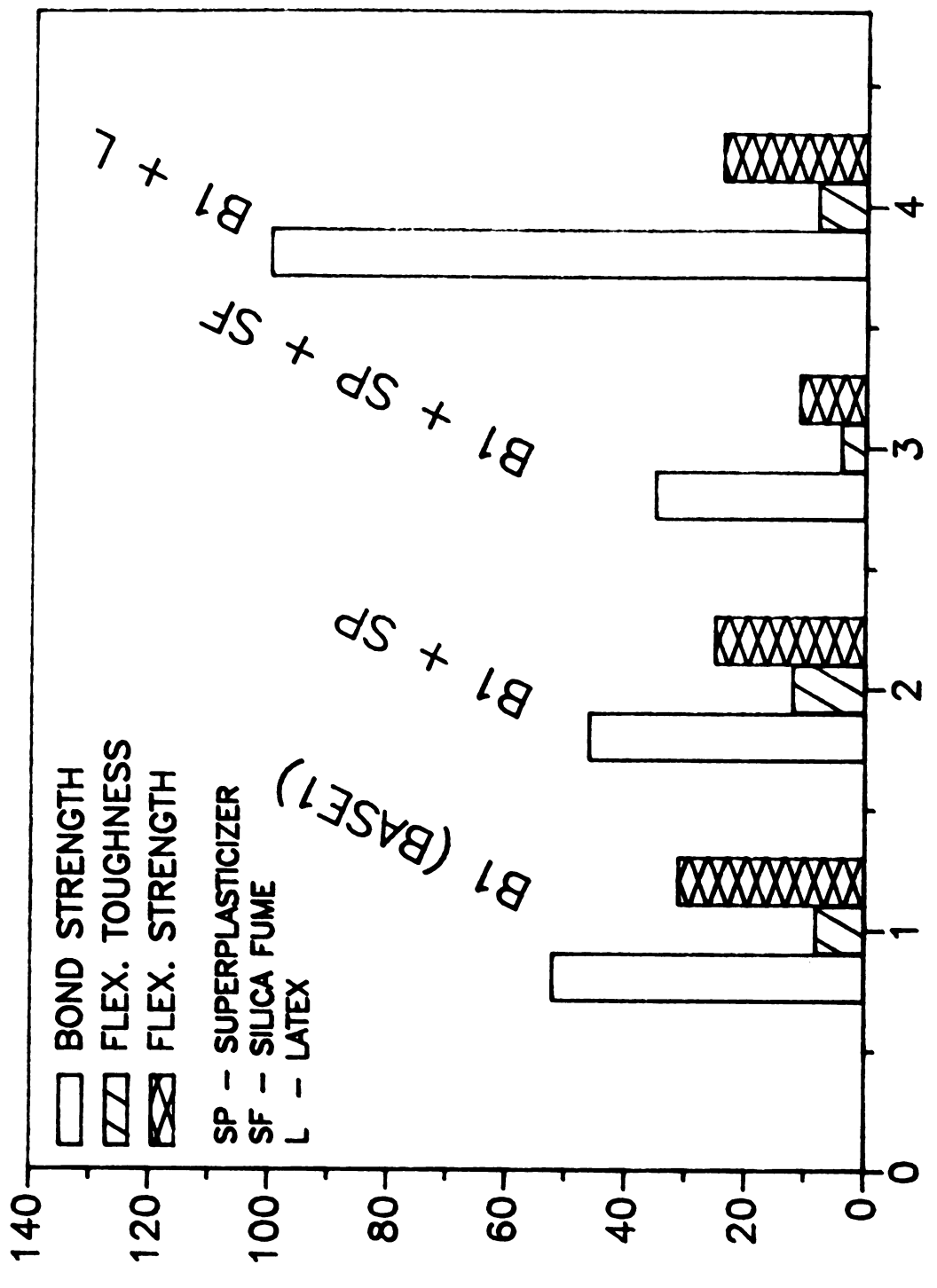

FIG. 10 PULL–OUT AND FLEXURAL SPECIMEN RESULTS

Figure 11 Carboflex Carbon Fiber "As Received"

Figure 12 Carbon Fiber Pulled Out of Mix 1

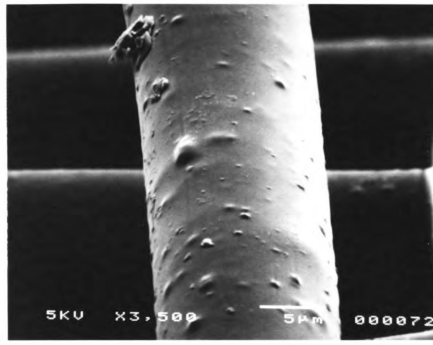
5KV X3,500 5µm 000072

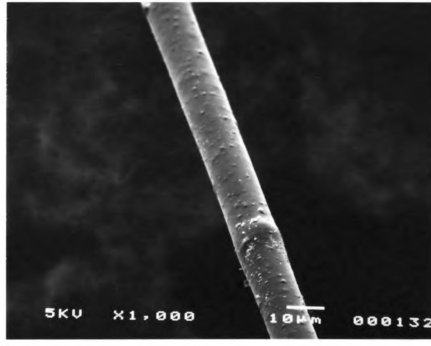
5KV X1,000 10µm 000132

Matrix property effects include increased workability with increased water content, but flexural strength and toughness decrease because of additional voids in the hydrated cement. These voids are created when excess water leaves the cement in the cure cycle.

SUPERPLASTICIZER Superplasticizer has a negligible effect on bond strength from comparison of mixes 1 and 2. Superplasticizers increase mix workability, so much less water was required to obtain comparable flow. The bond strength is dependant on workability, and these mixes have comparable workabilities, therefore the bond strength is expected to be nearly constant even though the water/cement ratio is very low for this mix.

The matrix was improved and made more consistent with the aid of the superplasticizer because the cement particles became more evenly dispersed. The average flexural strength was constant, but the standard deviation decreased in mix 2. Because cement is a flaw sensitive material, quite often the standard deviation in strength is large. The decrease in standard deviation with the use of superplasticizer is significant. The toughness increased slightly, which is expected with a more uniform matrix.

SILICA FUME Bond strength results for mixes 2 and 3 show that the addition of silica fume slightly decreased the bond strength. Silica fume is 100 times smaller than the fiber diameter, whereas the cement particle size is comparable to the fiber diameter. It was expected that the small silica fume particles would fill the interstices between fiber and cement particles producing better packing and fiber-matrix contact, thereby improving adhesion.

The matrix properties were decreased by the addition of silica fume. This may be the result of the acceleration of the cement hydration process and increased shrinkage. Because of the large surface area of silica fume, the amount of material available for reaction is dramatically increased compared with a cement mix without

silica fume. The acceleration of the hydration reaction causes the structure of the cement to be less than optimum, yielding poor matrix properties.

SEM pictures of the pulled out carbon fibers from mixes 2 and 3 (Figures 13 and 14) are very similar to mix 1 (Figure 12). They show that only a small amount of cement is adhering to the pulled out fibers, thus the failure mechanism is interfacial failure for mixes 1 through 3.

LATEX Comparison of the data generated on mixes 1 and 4 shows that latex produces a major improvement in the bond strength. Latex forms a film within the cement which increases the bonding between aggregate and cement. Therefore, it is logical to expect latex to improve the bond between carbon fiber and cement. Photographs show that there is a noticeable difference in the fiber-cement interface in mix 4 compared with mix 1. (Figure 15 shows a representative pull-out specimen fiber from mix 4, and Figure 16 is a close-up of the cement adhering to the fiber in Figure 15). The latex modified cement covers nearly half of the fiber surface. Thus, the failure mode is shifted from almost entirely interfacial failure, to interface and interphase failure. Interphase failure occurs when the fiber-cement interfacial shear bond strength is greater than the cement shear strength in the cement surrounding the fiber. Failure occurs in the weakest point through which load is transferred between the matrix and the fiber. For latex-modified cement, the fiber-matrix bond strength is sometimes greater than the cement shear strength in the cement surrounding the fiber.

Although the modulus of rupture decreased slightly with latex, the toughness remained the same. The modulus of rupture and toughness are expected to increase because of microcrack inhibition by latex. Anti-foam agent was not used with this mix, and the air void volume fraction was approximately 50%, creating a matrix with poor properties. A reduction in void volume fraction to 5%, would be expected to increase the strength of the cement by 100%.

Figure 13 Carbon Fiber Pulled Out of Mix 2

Figure 14 Carbon Fiber Pulled Out of Mix 3

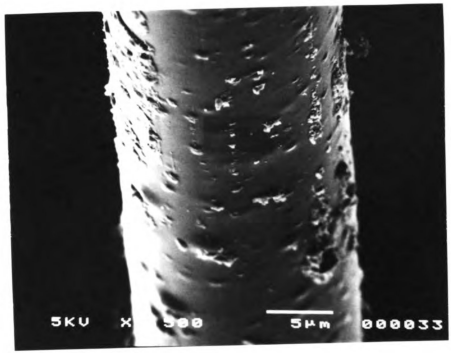
5KU
5μm
000033

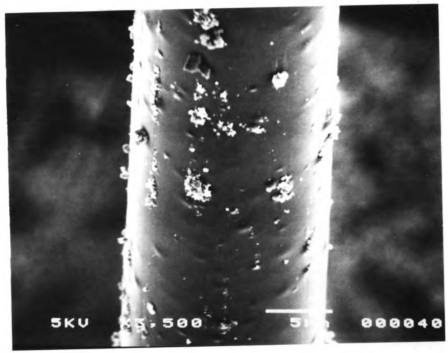
5KU
000040

Figure 15 Carbon Fiber Pulled Out of Mix 4

Figure 16 Close-Up of Latex-Modified Cement Adhered to Fiber

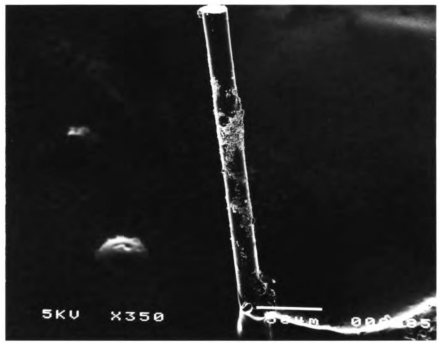
5KU X350

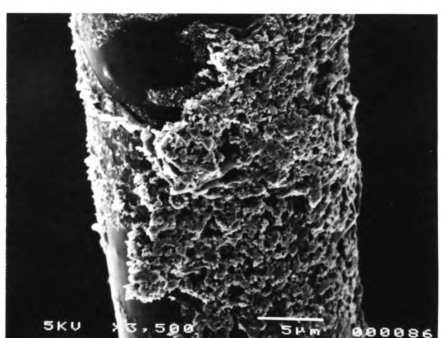
5KU
5µm
000086

PART II - MATRIX

The effect of five variables on the interfacial bond strength and matrix properties were determined in the second series of experiments. Table 6 shows the results of the experiments, and Figure 17 shows this data graphically. From this graph it is apparent that mixes 8 and 9 have properties superior to the other mixes. Typical normalized load-displacement curves for each of the mixes are shown in Figure 18. The load has been normalized to account for small variations in specimen size.

FIBER The effect of adding fiber to the matrix and the consequent improvement in matrix properties is evident from mixes 5 and 6. SEM photomicrographs of pulled-out fibers from mixes 5 and 6 show fiber coverage similar to mixes 1 through 3. Only a slight amount of cement was adhering to the fiber surface after fiber pull-out from either the pull-out or flexural specimen. The failure mode is interfacial failure in both of these mixes. The bond strength increases slightly as a result of the addition of fibers to the mix, because the fibers greatly improve the strength and stiffness of the matrix. When aggregates are added to cement, the matrix morphology is altered. It is unlikely that fibers induce an interphase similar to the transition zone found around aggregates where a water film is adsorbed on the aggregate surface. No water film will form on the fiber surface, because fibers are hydrophobic.

The matrix without fibers or aggregates (mix 5) develops shrinkage cracks visible to the unaided eye. This matrix is a very poor material with low strength and toughness. The addition of fibers inhibited the shrinkage cracks and drastically increased the modulus of rupture and toughness. Reduction of microcracking and shrinkage then are the probable causes of the bond improvement and results in an increase in the bond strength.

Table 6 Results of Pull-Out and Flexural Tests for Mixes 5 to 10

Mix#	Bond Strength	Toughness	Flexural Strength	Flexural Stiffness	W/B	Flow
	MPa (psi) %CV	Kg×mm (lb×in) %CV	MPa (psi) %CV	MPa/mm (ksi/in) %CV	%	%
5	3.2 (460) 20	10 (.86) 14	1.4 (210) 24	31 (115) 13	31.0	128
6	4.0 (580) 31	46 (4.0) 10	8.3 (1210) 4	38 (140) 25	31.0	117
7	NR	53 (4.6) 33	6.3 (920) 12	42 (155) 10	32.8	~0
7	NR 33	52 (4.5) 32	7.8 (1130) 16	42 (155) 16	34.1	37
7	4.8 (690) 13	44 (3.8) 26	8.3 (1200) 17	38 (140) 21	34.1	74
8	>5.9 (850)	48 (4.2) 19	11.8 (1710) 4	64 (235) 17	32.8	~0
9	3.8 (550) 42	92 (8.0) 15	11.7 (1700) 24	30 (110) 27	38.4	91
10	4.6 (670) 25	80 (6.9) 30	4.9 (710) 18	14 (50) 40	38.4	79

Key
W/B = Water to Binder Ratio
Flow = Result of Flow Test
%CV = Percent Coefficient of Variation

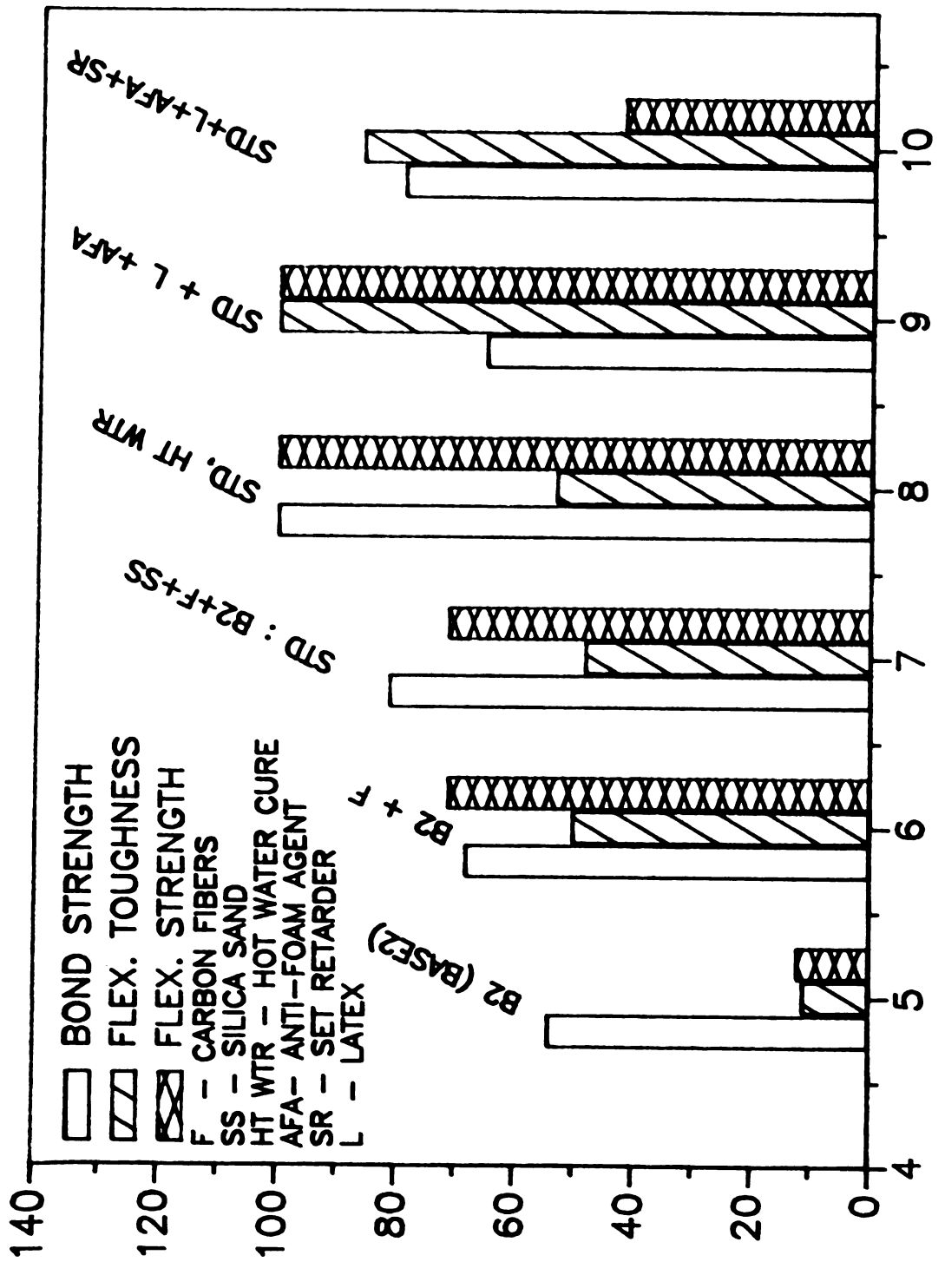

FIG. 17 PULL–OUT AND FLEXURAL SPECIMEN RESULTS

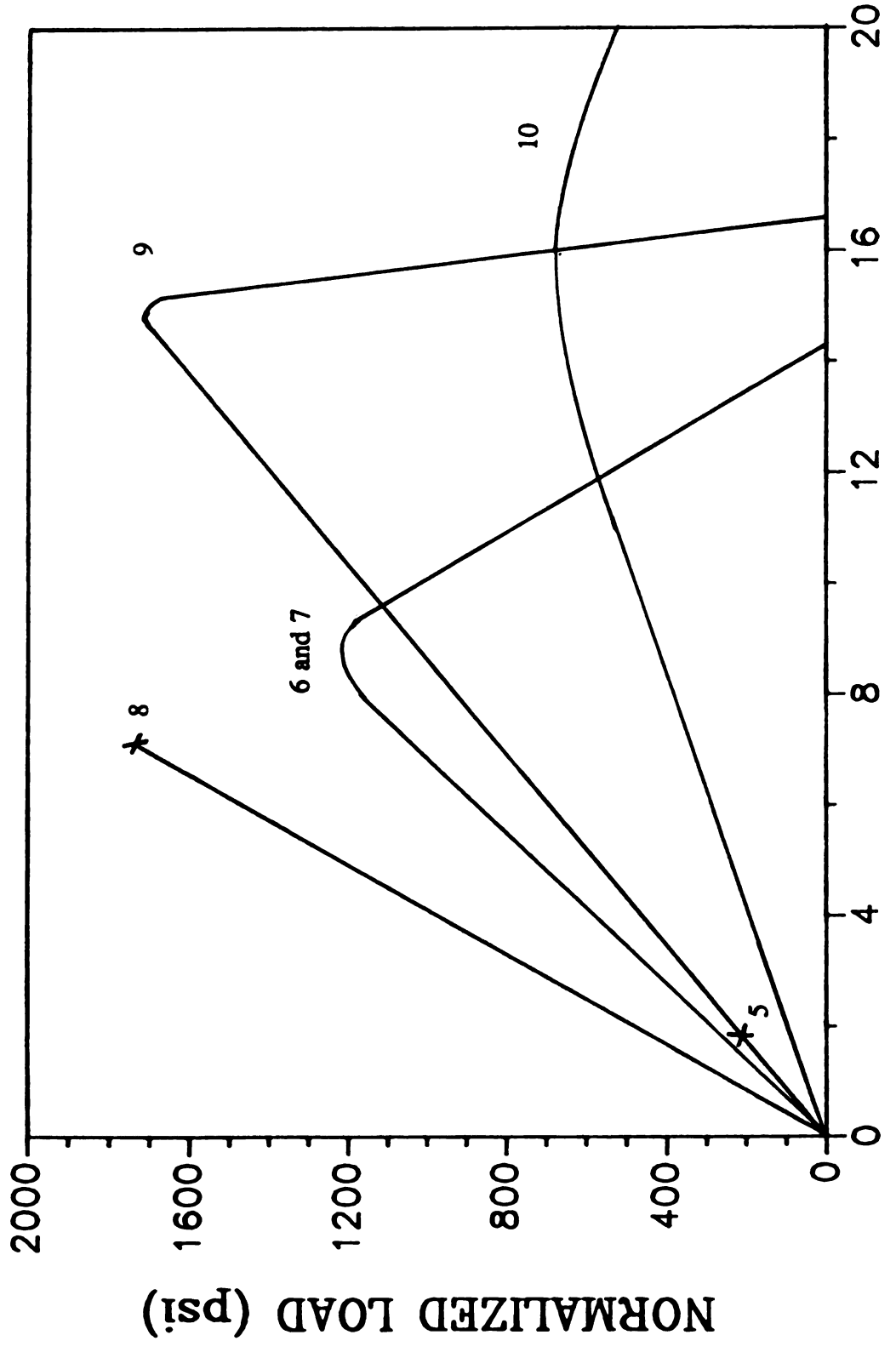

FIGURE 18 NORMALIZED LOAD VS. DISPLACEMENT

SILICA SAND The effect of silica sand on the CFRC interface is illustrated by studying the differences between mixes 6 and 7. The sand increases the bond strength slightly and alters the matrix morphology. The presence of a transition zone may be the source of the increased bond strength.

The matrix properties, however, are not affected by the addition of sand to CRFC. Cement should be restrained against shrinkage movements and its consequent cracking. In each of these mixes, the restraint is available, by fibers alone or by both fibers and sand.

The pull-out and flexural specimen carbon fiber surfaces show partial cement coverage of about 30%. Figure 19 shows a fiber from a pull-out specimen from mix 7, and Figure 20 shows a flexural specimen fracture surface from mix 7. The cement particles adhering to both specimens are less than 5 microns, and many of the adhering particles are approximately 1 micron in diameter.

It is very important to the validity of the pull-out test that the surfaces of the pull-out and flexural specimen carbon fibers be very similar. Figures 19 and 20 show that the interfaces for the two specimen types are nearly the same. The cement mixing process pushes the carbon fibers into contact with the cement mix in making a CFRC flexural specimen. There is no such action between the fibers of a fiber holder and the cement mix in making a pull-out specimen. Because the fiber surfaces appear to be similar, the pull-out test is assumed to be a good model to the fiber pull-out which occurs in a flexural specimen.

HOT WATER CURING Mixes 7 and 8 show the increase in bond strength caused by hot water curing. For mix 8 no critical length could be measured, all the fibers in the pull-out specimen ruptured. The interfacial bond strength is recorded as being greater than the bond strength associated with the smallest fiber embeddment length which was routinely produced (0.6 mm). Figure 21 shows that the failure was completely the result of fiber fracture, representative of "perfect" bonding. There are

Figure 19 Carbon Fiber Pulled Out of Mix 7

Figure 20 Flexural Specimen Fracture Surface of Mix 7

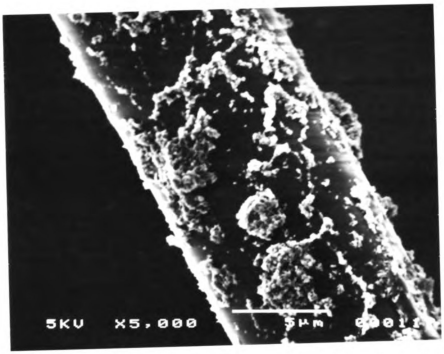
5KV X5,000
5µm

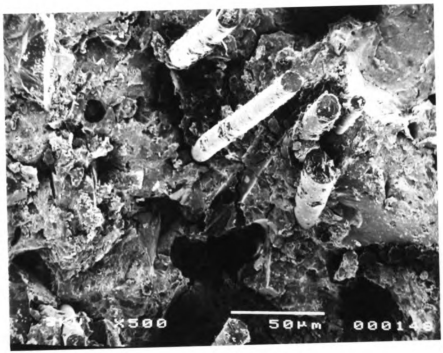
X500
50µm 0001

no pulled out fibers on the fracture surface.

Figure 22 shows that only a slight amount of cement is adhering to the fiber. The exposed fiber lengths are on the order of several fiber diameters, and the fibers have fractured ends. Thus, the debond length is expected to be on the order of several fiber diameters. Once an area of the fiber is debonded, the stress in that portion of the fiber is very near the stress in the portion of the fiber bridging the crack. Frictional bonding will cause the stress in the debonded region to be less than the stress in the crack bridging portion of the fiber.

When the CFRC failure mechanism is fiber rupture, failure will typically occur at a flaw in the fiber. If a flaw is present in the crack bridging portion or the debonded region of the fiber, fiber failure will occur at the flaw. Figure 22 shows the fracture surface resulting from fiber failure in the debonded region of the fiber. This photograph also shows fiber-matrix debonding as indicated by a gap which exists between the fibers and the matrix at the fracture surface. Thus, when the CFRC failure mechanism is fiber rupture, debonding occurs.

Cracks are eminating from the fibers in Figure 22. This type of cracking may be a major mechanism of energy absorption. Some of the energy of the main crack is diverted to small cracks in various directions. Diversion of the large crack's energy is essential to restraining it. Thus, the propagation of the main crack is inhibited by carbon fibers. (This cracking is not a by-product of the SEM specimen preparation. Fibers were placed into a cement sample to give the same geometry as is shown in Figure 22. When this sample received the SEM specimen preparation no cracking near the fibers occured. Thus the cracks eminating from the fibers in Figure 22 are the result of the failure mechanism in the CFRC.)

The curing schedule of mix 8 caused the CFRC strength to increase 80% over the same cement batch which was cured at room temperature. The hydration reaction was accelerated by the high temperature and high water pressure. Silica fume

Figure 21 Carbon Fiber Pulled Out of Mix 8

Figure 22 Flexural Specimen Fracture Surface of Mix 8

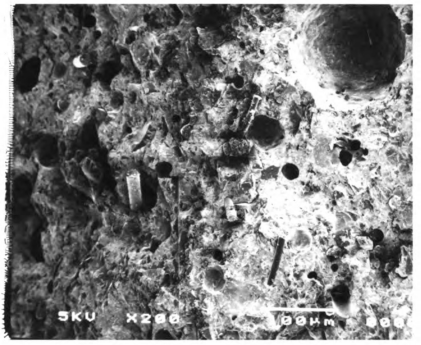
5KU X200

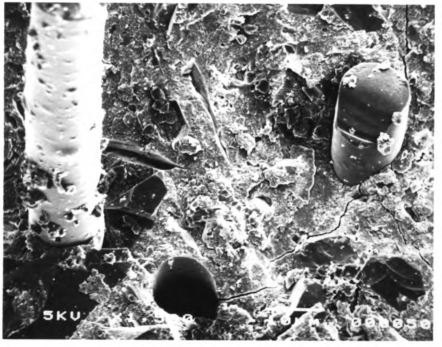
5KU

increased the strength gain because of silica fume's large surface area and reactivity.

The toughness (area under the curve) of the mixes 7 and 8 are the same, as shown by Figure 18. The normalized load-displacement curve of mix 7 shows that it has more ductility than mix 8, and a small "plastic" region. The normalized load-displacement curve for mix 8 is linear until catastrophic failure, when the strength becomes zero. Thus, although the toughnesses of the mixes are the same, the failure modes are completely different. Fibers pull-out and fracture in mix 7, whereas in mix 8 the failure mechanism is entirely fiber fracture.

LATEX AND ANTI-FOAM AGENT The measurements completed on mixes 4, 7, and 9 show that anti-foam agent is interfering with the bonding provided by latex in the CFRC. Mixes 7 and 9 differ only in that mix 9 contains latex and anti-foam agent. Because of the inclusion of latex, the bond strength of mix 9 was expected to be similar to that of mix 4. The bond strength increases, but less than expected. Hence, it is suspected that the anti-foam agent is responsible for interfering with the bond strength. Anti-foam agent is a surfactant which lowers the surface tension of the mix. Although it is expected to increase contact between the mix and the fibers, the molecule is non-polar and no hydrogen bonding is expected to this molecule.

The exposed lengths of the fibers on the flexural specimen fracture surface are on the order of several fiber diameters, as shown by Figure 23. Figure 24 shows a typical size of cement adherend (greater than 5 microns in diameter). Comparison of Figure 15 (mix 4) and Figure 24 (mix 9) shows that the mixes with latex have similarly large adhered cement particles. Both of the figures show that the fiber surface not covered by the large particles is nearly free of cement. The inhomogeneity of the cement matrix is responsible for the variations in the fiber-matrix bonding.

Figure 23 Carbon Fiber Pulled Out of Mix 9

Figure 24 Flexural Specimen Fracture Surface of Mix 9

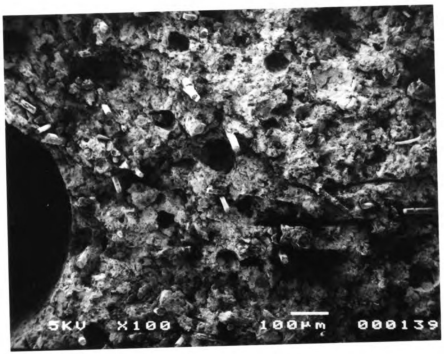
5KV X100 100µm 000139


5KV X1,500 10µm 000141

Figure 24 shows a representative ruptured carbon fiber. The failure mechanism of mix 9 involves fiber rupture and bridging of microcracks by latex. The strength and toughness values of this mix are the highest of all the mixes. The strength increase is the result of crack inhibition by latex. Latex bridges microcracks, slowing their growth. The high energy absorption of this mix is also linked to the action of latex bridging cracks. The increase in strength and ductility from mix 7 to mix 9 is the result of this failure mechanism. Latex and anti-foam agent cause a substantial increase in the strength and toughness of CFRC.

SET RETARDER Set retarder causes the bond strength to increase. Mix 10 has a higher bond strength than mix 9. This is expected because set retarder coats the cement particles and the fibers, slowing the hydration of the cement. This coating acts as a coupling agent between the matrix and the fiber, yielding good adhesion.

Set retarder decreased the latex-modified CFRC flexural strength by 60%, and caused a 10% loss of toughness. Set retarder increases the strength of normal cement after the second day. Thus, the set retarder has interacted with one of the admixtures, probably latex. The set retarder is typically deactivated after 24 hours, allowing hydration to continue at an increased rate. The latex could prolong the retarding effect by holding the set retarder at the cement particle surface well beyond 24 hours.

GENERAL RESULTS

The fiber-matrix bond strength is dependent on the matrix as well as the interface. The bond strength is plotted against flexural stiffness of the composite materials without latex in Figure 25. This relationship shows the effect of the different admixtures on the bond strength and the CFRC flexural stiffness. As the bond strength increases because of improved mechanical interlocking, the transfer of

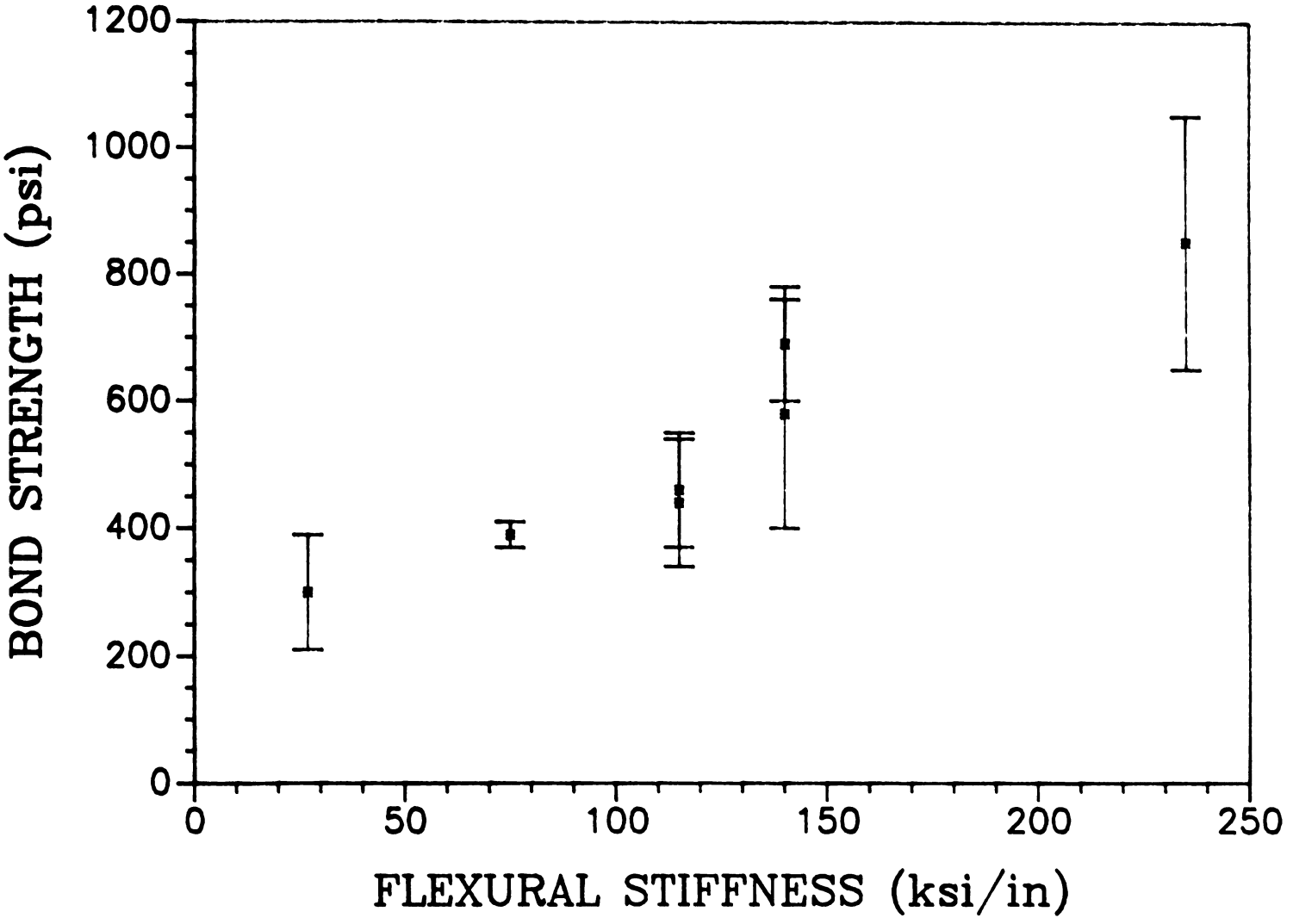

FIGURE 25 BOND STRENGTH VS. FLEX. STIFFNESS

stress from the matrix, through the interface, to the fiber improves. The CFRC flexural stiffness for mixes without latex is dependent on the average fiber-matrix interfacial shear bond strength.

SUMMARY AND CONCLUSIONS

PART I - INTERFACE

The average carbon fiber-cement interfacial shear bond strength is increased by increasing the water-binder ratio in a simple cement mix. The increase is attributable to an improvement in workability (i.e. better fiber-matrix contact is achieved). The addition of superplasticizer to this mix does not affect the bond strength.

The average carbon fiber-cement bond strength is decreased by the addition of silica fume to a simple cement mix. Silica fume improves CFRC flexural strength and toughness indirectly by improving fiber dispersion, but does not specifically alter fiber-matrix adhesion.

The addition of latex to a simple cement mix dramatically increases the carbon fiber-cement bond strength. The latex acts as a coupling agent between the fiber and the matrix, providing excellent physical contact between the carbon fibers and cement.

PART II - MATRIX

Two techniques improved the flexural strength of silica fume-modified CFRC by 40%. The addition of latex and anti-foam agent to silica fume-modified CFRC increases its flexural strength and flexural toughness by detering crack propagation.

Hot water curing silica fume-modified CFRC dramatically increases the carbon fiber-cement bond strength, flexural strength, and flexural stiffness.

Silica sand causes a slight increase in the average carbon fiber-cement interfacial shear bond strength by improving the cement matrix. The dimensional stability provided by silica sand reduces shrinkage microcracking, thus improving the matrix.

Anti-foam agent inhibits carbon fiber-cement adhesion by producing a film on the fibers which limits secondary interactions between the phases.

The addition of set retarder to latex-modified cement has an undesirable effect, because latex interacts with the set retarder, keeping the cement from hydrating. The set retarder is held at the cement particle surface by the latex, preventing the material strength from developing to the level it does in cement without set retarder.

GENERAL

Admixtures (excluding latex) which increase CFRC flexural stiffness also increase carbon fiber-cement adhesion.

Increases in fiber-matrix adhesion change the failure mechanism observed in CFRC from both fiber pull-out and fracture to complete fiber fracture. This increases the CFRC flexural strength substantially, but only slightly increases toughness.

Both hot water curing and the addition of latex with anti-foam agent to CFRC yield optimum flexural strength. Latex-modified CFRC has optimum flexural toughness, and hot water cured CFRC has optimum flexural stiffness.

APPENDIX

APPENDIX A CFRC MIXING PROCEDURE

1. Weigh out all constituents (all liquids together).

2. All utinsels and mixing apparatus must be clean. Wet the surfaces which will contact cement with water, then allow them to drip for 30 seconds.

3. Place silica fume in mixer if present. If not, add half of cement.

4. Add 2/3 of liquids.

5. Cover top of mixer with plastic.

6. Turn mixer on speed 1 for 40 seconds.

7. Add fibers (if present) slowly (no clumping).

8. Add silica sand (if present) slowly with water as required.

9. Add cement as rapidly as it can be mixed in, alternating with the rest of the water.

10. Turn mixer off.

11. Switch to speed 2 for 2 minutes.

12. Pour into molds.

13. Vibrate for 10 seconds. Wear ear protection!

14. Do flow table test in accordance with ASTM C230 "Flow Table for use in Tests of Hydraulic Cement" 1 minute after the mixer is shut off.

APPENDIX B CALCULATIONS

MIX DESIGN

Vm = total volume of the cement mix
Si = specific volume of constituent i
Mi = mass of consitituent i
B = mass of cementitious material (binder) = mass of cement + silica fume

The mix design uses mass ratios of constituents to binder (Mi/B), therefore, once the mass of the binder (B) is known, the mass of constituents (Mi) are easily obtained by multiplying the ratio by B. B is calculated as follows:

$Vm = \Sigma(MiSi)$

Take the sum for all constituents (i).

$Vm = B \Sigma(MiSi/B)$

$B = Vm \div \Sigma(MiSi/B)$

MODULUS OF RUPTURE

See ASTM C78-84, Flexural Strength of Concrete (Using Simple Beam With Third-Point Loading), for the conditions under which the following equation is valid.

R = modulus of rupture
P = maximum applied load
L = span between bottom two load points
b = average width of specimen
d = average depth of specimen

$R = 1.5PL/bd^2$

FLEXURAL STIFFNESS

The flexural stiffness is the initial slope of the normalized load vs. displacement curve (Figure 18). The normalized load is calculated in the same manner as the modulus of rupture, but instead of the maximum applied load, the applied load for the given displacement is used.

LIST OF REFERENCES

LIST OF REFERENCES

1. Coutts, R.S.P., "Sticks and Stones...!!," *Forest Products Newsletter*, CSIRO Division of Chemical and Wood Technology (Australia), **2**, no. 1, Jan. (1988), pp 1-4.

2. Mindess, S., Young, J.F., *Concrete* (Englewood Cliffs, N.J.: Prentice-Hall, Inc., 1981), pp 76-86.

3. Mindess, S., Young, J.F., pp 77-80

4. Mindess, S., Young, J.F., pp 312-19

5. Mindess, S., Young, J.F., pp 89

6. Mindess, S., Young, J.F., pp 88-92

7. Mindess, S., Young, J.F., pp 382-85

8. Mindess, S., Young, J.F., pp 385-88

9. Maso, F., *Proceedings of the Seventh International Congress on the Chemistry of Cements*, **1**, Paris (1980).

10. Mindess, S., Young, J.F., pp 353-366

11. Mindess, S., Young, J.F., pp 364-371

12. "State-of-the-Art Report on Fiber Reinforced Concrete," Rept# ACI 544, 1R-82, Concrete International, pp 11.

13. Wang, Y., Backer, S., and Li, V.C., "An Experimental Study of Synthetic Fiber Reinforced Cementitious Composites," *Journal of Materials Science*, **22**, (1987), pp 4281.

14. Akers, S.A.S., and Garrett, G.G., "Fiber-matrix Interface Effects in Asbestos-cement Composites," *Journal of Materials Science*, **18**, (1983), pp 2200-2208.

15. Akers, S.A.S., and Garrett, G.G., International Journal of Cement Composites and Lightweight Concrete, 5:173, (1983).

16. Gray, R.J., "Fiber-matrix Bonding in Steel Fiber Reinforced Cement-Based Composites," *Proceedings of the Fourth International Symposium on the Fracture Mechanics of Ceramics*, June (1985), Blacksburg, Virginia, pp 53-66.

17. Bayasi, Z., and Soroushian, P., "Silica Fume Effects on the Pull-Out Behavior of Randomly Oriented Steel Fibers From Concrete", *Bonding in Cementitious Composites*, S. Mindess and S.P. Shah, Eds, Materials Research Society Symposium Proceedings, **114**, December (1987), Boston, Massachusetts, pp 187-196.

18. Gopalaratnam, V.S., and Abu-Mathour, H.J., "Investigation of the Pull-out Characteristics of Steel Fibers from Mortar Matrices," Proceedings of the International Symposium on Fiber Reinforced Concrete, December 16-19 (1987), Madras, India, pp 2.201-2.211.

19. Gray, R.J., and Johnston, C.D., "The Effects of Matrix Composition of Fiber/Matrix Interfacial Bond Shear Strength in Fiber-Reinforced Mortar," *Cement and Concrete Research*, **14**, (1984), pp 285-296.

20. Gray, R.J., "Analysis of the Effect of Embedded Fibre Length on Fibre Debonding and Pull-Out from an Elastic Matrix", *Journal of Materials Science*, **19**, (1984), pp 1680-1691.

21. Bentur, A., "Interfaces in Fiber Reinforced Cements," *Bonding in Cementitious Composites*, Materials Research Society Symposium Proceedings, **114**, December (1987), Boston, Massachusetts, pp 133-144.

22. Kawamura, M., Igarashi, S., and Hasaba, S., "Durability of Glass Fiber Reinforced Mortar and Concrete", Proceedings, *International Symposium on Composite Material Structures*, (1986), pp 1116-121.

23. Odler, I., "Structure and Mechanical Properties of Portland Cement-Polyacrylonitrile Fiber Composites," *Bonding in Cementitious Composites*, Materials Research Society Symposium Proceedings, S. Mindess and S.P. Shah, Eds, **114**, December (1987), Boston, Massachusetts, pp 153-58.

24. Majumdar, A.J., RILEM Symposium on Fiber Reinforced Cement and Concrete, **1**, September (1975), ed. A. Neville, Construction Press Ltd., London, pp 279-313.

25. Wang, Y., Backer, S., and Li, V.C., pp 4281-4291.

26. Walton, P.L., and Majumdar, A.J., "Properties of Cement Composites Reinforced with Kevlar Fibers," *Journal of Materials Science*, **13**, (1978), pp 1075-83.

27. Coutts, R.S.P., and Kightly, P., "Bonding in Wood Fiber-cement Composites," *Journal of Materials Science*, **19**, (1984), pp 3355-59.

28. Akihama, S., Suenaga, T., and Nakagawa, H., "Carbon Fiber Reinforced Concrete," *Concrete International*, January (1988), pp 40-47.

29. Bayasi, Z., "Carbon Fiber Reinforced Cement", Ph.D. Thesis, Michigan State University, (1988).

30. Ohama, Y., and Amano, M., "Effects of Silica Fume and Water-Reducing Agent on Properties of Carbon Fiber Reinforced Mortar," *Proceedings of the 27th Japanese Congress on Materials Research*, (1984), pp 187-191.

31. Nagi, M., and Sorousian, P., "Carbon Fiber Reinforced Cement Cladding Panels: Material Development, Construction and Design," Michigan State University, June (1988), pp 3-8.

32. Ohama, Y., Demura, K., Sato, Y., "Development of Lightweight Carbon Fiber Reinforced Fly Ash-Cement Composites," *Proceedings of the International Symposium of Fiber Reinforced Concrete*, December (1987), Madras, India, pp 3.23-3.31.

33. Bayasi, Z., "Carbon Fiber Reinforced Cement", Ph.D. Thesis, Michigan State University, (1988).

34. Bartos, Peter, "Review Paper: Bond in Fiber Reinforced Cements and Concretes", *The International Journal of Cement Composites*, **3**, no. 3, August (1981), pp 159-177.

35. Nishioka, K., Yamakawa, S., and Shirakawa, K., "Properties and Applications of Carbon Fiber Reinforced Cement Composites," Proceedings, *RILEM Symposium on Developments in Fiber Reinforced Cement and Concrete*, RILEM Technical Committee 49-TFR, Sheffield, July, (1986).

36. Akihama, S., Suenaga, T., Nakagawa, H., Suzuki, K., "Influences of Fiber Strength and Polymer Impregnation on the Mechanical Properties of Carbon Fiber Reinforced Cement Composites," Proceedings, *RILEM Symposium on Developments in Fiber Reinforced Cement and Concrete*, RILEM Technical Committee 49-TFR, Sheffield, July, (1986).

37. Ashland Carbon Fiber Division, "Ashland Product Information Sheets: Carboflex", Ashland Chemical Company, Ashland, KY, (1985).

38. "Price List for Standard THORNEL Pan Fibers," Amoco Performance Products, Inc., 38-C Grove Street, Ridgefield, CT, 06877, Price List Effective September 1, 1988.

39. Akihama, S., Suenaga, T., and Banno, T., "Mechanical Properties of Carbon Fiber Reinforced Cement Composites," *The International Journal of Cement Composites and Lightweight Concrete*, **8**, no. 1, February (1986), pp 21-33.

40. Kamakura, M., et al., "Mechanical Properties of Carbon Fiber Reinforced Cement (CFRC)", *Sumitomo Metals*, Kinzoku, Japan, **34**, no. 4, December (1982), pp 69-78.

41. Akihama, S., Suenaga, T., and Banno, T., "The Behaviour of Carbon Fiber Reinforced Cement Composites in Direct Tension," *International Journal of Cementitious Composites and Lightweight Concrete*, **6**, (1984), pp 159-168.

42. Bayasi, Z., "Carbon Fiber Reinforced Cement", Ph. D. Thesis, Michigan State University, (1988).

43. Ohama, Y., "Principle of Latex Modification and some Typical Properties of Latex-Modified Mortars and Concretes," *American Concrete Institute Materials Journal*, Title No. 84-M45, Nov.-Dec. (1985), pp 511-18.

44. Mindess, S., Gray, R.J., "Bonding in Cementitious Composites: How Important is it?", *Bonding in Cementitious Composites*, Materials Research Society Symposium Proceedings, S. Mindess and S.P. Shah, Eds, **114**, December (1987), Boston, Massachusetts, pp 5-12

45. Ohama, Y., Demura, K., Sato, Y., pp 3.23-3.31.

46. Ohama, Y., Amano, M., and Endo, M., "Properties of Carbon Fiber Reinforced Cement with Silica Fume," *Concrete International*, March (1985), pp 58-62.

47. Bayasi, Z., "Carbon Fiber Reinforced Cement", Ph. D. Thesis, Michigan State University, (1988).

48. Unimin Corporation, Troy Grove, Illinois.

49. Guennewig, T., "Cost-Effective use of Superplasticizers, "*Concrete International*, March (1988), pp 31-34.

50. Elkem Chemical, Inc., Production Information Brochures on Microsilica Additives, Pittsburg, Pennsylvania, (1986).

51. Mindess, S., Young, J.F., pp 76-80.

52. Morgan, D.R., "Dry-Mix Silica Fume Shotcrete in Western Canada," *Concrete International*, January (1988), pp 24-32.

53. Ashland Carbon Fiber Division, "Ashland Product Information Sheets: Carboflex", Ashland Chemical Company, Ashland, KY, (1985).

54. Ohama, Y., pp 511-18.

55. Private Conversation with Mr. P. Pape, Dow Corning, June 1, 1988.

56. Private Conversation with Mr. Devantier, W.R. Grace & Company, June 27, 1988.

57. Narkis, M., Chen, E.J.H., "Review of Methods for Characterization of Interfacial Fiber-Matrix Interactions," *Polymer Composites*, **9**, no. 4, August (1988), pp 245-251.

58. Gray, R.J., "Experimental Techniques for Measuring Fibre/Matrix Interfacial Bond Shear Strength", *International Journal of Adhesion and Adhesives*, **3**, no. 4, October (1983), pp 197-202.

59. Wang, Y., Backer, S., and Li, V.C., pp 4283-84.

60. Thornton, P.R., *Scanning Electron Microscopy*, (New York, N.Y., Chapman and Hall LTD., 1968), pp 15-22.

61. Briggs, D., Seah, M.P., *Practical Surface Analysis by Auger and Photo-Electron Spectroscopy*, (New York, N.Y., John Wiley & Sons, Inc., 1983), pp 5-23.